


## Article

# An Innovative Photovoltaic Luminescent Solar Concentrator Window: Energy and Environmental Aspects

Vincenzo Muteri <sup>1</sup>, Francesco Guarino <sup>1</sup>, Sonia Longo <sup>1,\*</sup> , Letizia Bua <sup>2</sup>, Maurizio Cellura <sup>1</sup>, Daniele Testa <sup>2</sup> and Marco Bonzi <sup>2</sup>

<sup>1</sup> Department of Engineering, University of Palermo, 90128 Palermo, Italy; vincenzo.muteri@unipa.it (V.M.); francesco.guarino@unipa.it (F.G.); maurizio.cellura@unipa.it (M.C.)

<sup>2</sup> Eni S.p.A., Renewable Energy, Magnetic Fusion and Material Science Research Center, 28100 Novara, Italy; letizia.bua@eni.com (L.B.); daniele.testa@eni.com (D.T.); marco.bonzi@eni.com (M.B.)

\* Correspondence: sonia.longo@unipa.it; Tel.: +39-091-23861927

**Abstract:** Over the years, different types of smart windows have been tested and developed. In this study, an innovative prototype of a photovoltaic smart window, that integrates luminescent solar concentrators, was analysed. The device independently regulates the movement of the shading system and allows energy surplus, through the electricity generated by modules. Considering the peculiar structure (characterized by the presence of a light shelf) and the thermal characteristics of the device, the analyses focused on optical, thermal, and electrical performances, comparing them with those of a traditional window. The analysis followed an experimental approach that involved lighting and electrical monitoring studies in a real test room, to create validated models for conducting simulations in larger buildings. The results were expressed through the study of illuminance maps, electricity generation obtainable from the integrated photovoltaic technology and in terms of energy savings. Energy generation accounts for around 10 Wh/month, with up to 50% improvement from the perspective of energy use for heating and cooling. The technology proves effective in allowing efficient overall energy performances while generating enough energy to operate the smart window control systems.

**Keywords:** smart window; LSC; BIPV; energy saving; LCA; office building



**Citation:** Muteri, V.; Guarino, F.; Longo, S.; Bua, L.; Cellura, M.; Testa, D.; Bonzi, M. An Innovative Photovoltaic Luminescent Solar Concentrator Window: Energy and Environmental Aspects. *Sustainability* **2022**, *14*, 4292. <https://doi.org/10.3390/su14074292>

Academic Editors: José Dinis Silvestre, Domenico Mazzeo and Zsuzsa Szalay

Received: 27 February 2022

Accepted: 30 March 2022

Published: 4 April 2022

**Publisher's Note:** MDPI stays neutral with regard to jurisdictional claims in published maps and institutional affiliations.



**Copyright:** © 2022 by the authors. Licensee MDPI, Basel, Switzerland. This article is an open access article distributed under the terms and conditions of the Creative Commons Attribution (CC BY) license (<https://creativecommons.org/licenses/by/4.0/>).

## 1. Introduction

Buildings are one of the largest single contributors to greenhouse gas emissions (36% of CO<sub>2</sub> emissions in the EU) [1,2]. In addition, the building sector accounts for about 40% of global primary energy consumption and, moreover, some factors such as growth of population, migration of people from rural to urban areas, changes in routine and lifestyle, could potentially further contribute to an increase in building energy use [3]. In the residential sector, the use of energy is related to heating and cooling of indoor environments, lighting, and other needs. All these aspects are influenced by factors such as building location and envelope energy performances, weather conditions, type and efficiency of equipment, access to energy, availability of energy sources, energy policies and lifestyle of the occupants. In the commercial sector, the energy use is mainly related to heating and water heating systems, cooling, lights, and other equipment strictly connected to the activity that is carried out inside the building [4]. Consequently, it is important to evaluate different strategies that could allow energy savings and better management of the thermal loads inside the buildings, both in commercial and residential ones.

Thanks to the new targets that the European Union has set for 2030 about energy and climate (40% cuts in greenhouse gas emissions, 32% share for renewable energy and 32.5% improvement in energy efficiency) the process of increasing energy saving has taken a central role for the correct design of buildings [5,6], in recent years. In fact, by adjusting properly solar radiation availability inside the rooms, it is possible to reduce the

energy consumption for lighting, cooling, and heating and, at the same time, maximize the comfort for the occupants; in this contest, the window represents a key element to achieve these goals.

Moreover, the building sector is particularly energy-intensive considering both the embodied energy and the operational phase energy use. The actual challenge is to go towards Positive Energy Buildings (PEBs) [7], producing more energy than necessary and supporting other buildings connected to them (positive energy districts) [8]. To achieve this result, it is necessary to also approach the on-site energy generation [9].

Windows are a critical element in the envelope: their sizing is one of the most critical issues within building energy performances, can cause high thermal losses, overheating and glare problems [10]. However, if designed correctly, they play an important role in improving indoor thermal comfort [11,12] and can also become active elements, being able to contribute to the on-site energy generation.

For the energy generation in buildings, photovoltaic (PV) technology represents today one of the best solutions. However, excluding the third photovoltaic generation that promises new types of installation, the exploitation of building roofs alone is not enough, as the energy supplied by the photovoltaic on roofs is limited by space and is sufficient only for small buildings. This contrasts to an urban context that points to buildings that will be taller and self-sufficient.

In this context, the study aims to investigate the performances of an innovative PV technology, Luminescent Solar Concentrator (LSC), integrated to a window through experimental studies. The contribution of the paper lies in the analysis of the innovative design of the window system, the statistical modelling of the energy generation it provides, the integrated environmental and energy performance analysis extended to its life cycle.

The results will be expanded further through the analysis of daylight and thermal performances of the device and the comparison of the results with those of a traditional window in the same conditions (room size and structural characteristics, measurement period, etc.).

## 2. State of the Art

The Smart Window—Luminescent Solar Concentrator) (SW-LSC)—incorporates the advantages of electricity generation from photovoltaic modules, and luminescent solar concentrators with the functionality of a smart window, which manage heat loads through an autonomous and passive shading system (motorized venetian blind).

The existing PV technologies can be classified into three generations according to their technical characteristics: Si based PV is the technology used for first-generation. Second-generation PV cells are usually manufactured by thin-film PV technology. Compared to the first-generation cells, they are usually made of very thin layers of semiconductor materials. Finally, the third-generation PV cells aims to produce more efficient and low-cost devices [13] by using new materials like perovskite, inks, nanotubes, organic dyes, etc. [14]. The LSC technology that is integrated into the smart window falls in this last type.

In this section, authors collected and examined studies that can be classified in two categories:

- Photovoltaic technologies integrated with buildings (BIPV), in particular semi-transparent PV (STPV) that allow PV panels to be placed in substitution of surfaces like façades or skylights;
- Smart windows, including the main categories as electrochromic, photochromic and thermochromic.

### 2.1. Semi-Transparent PV

The evolution of the STPV technologies has allowed applications previously only covered by traditional glass (skylights, windows, glass facades). For this reason, in addition to the generation of electricity, aspects such as solar heat gain reduction and day-lighting play an equally important role in assessing the effective efficiency of the devices in interior

spaces. For these devices, it is often essential to find a compromise between the higher energy generation and potential increase in lighting energy use. In fact, due to their structure, STPV technologies create areas of shade, which depend on the degree of visible transmittance of these devices, on the window-to-wall ratio (WWR), and which have consequences on the daytime illuminance factor and on the thermal balance of the environment.

An evaluation of one of these technologies was discussed by Sun et al. [15], who analysed the energy and daylight performances of a Cadmium Telluride (CdTe) PV glazing integrated into windows. The simulation was conducted through Energy Plus; the simulation related to a private office occupied by two people from 8.00 to 17.00 on weekdays. The annual energy performance of the PV window was calculated for an office under five different climatic conditions in China; the results were then compared to a conventional double glazing (DG) system. The most significant energy saving potential (73% under the tested climates) was obtained when covering 80% of the window area by PV glazing for 75% WWR. The study followed an approach like that of our work, in terms of final objectives, but there were no experimental tests conducted in the field in order to obtain real data by which to compare the results of the simulations. Furthermore, although the type of installation was the window, the technology analysed was different from that of luminescent solar concentrators.

Kapsis and Athienitis [16] evaluated the potential benefits of STPV in a cooling dominated commercial building located in Toronto. Those authors considered three different models for the evaluation of the performances of the STPV window: a day-lighting, an electrical and a thermal model. In addition, they investigated the impact of several design parameters (WWR, façade orientation, etc.) and different PV cell technologies. All results were expressed as a function of the visible effective transmittance of the STPV module (10%, 20%, 30%, 40%, 50%): the use of a STPV module with 10% visible effective transmittance (STPV-10%) was associated with the lowest annual electricity consumption (as low as 5 kW h/m<sup>2</sup>/yr), when the STPV annual electricity production was taken into account. In contrast, when excluding STPV electricity production, the authors found that the selection of STPV-Sh20% resulted in the most energy-conserving design. A limitation of the study was that no consideration was made regarding the type of integration into the building, in particular on some aspects such as window frames or window structure.

Although the purpose of the above studies was connected to our work, in some cases an experimental approach with direct measurements in the field was lacking while, in other cases, the aspects related to the way of integration in the building or the details on the characteristics of windows were neglected. To conclude, studies have not explored the aspects related to day-lighting that play a particularly central role for this type of technology.

## 2.2. Smart Windows

Smart windows are usually defined as a category of glass (smart glass) or other transparent materials whose light transmission properties change following the application of electrical voltage (electrochromism), light (photochromism), or heat (thermochromism). These technologies can be classified as active (thermochromic and photochromic) or passive (electrochromic). In comparison to traditional windows, smart windows can adjust their optical properties in response to the modification of some boundary variables and hence have the potential to improve the energy performance of buildings and the comfort of the residents, thanks to their dynamic and adaptive functioning. Therefore, the aim of dynamic glazing systems is to control incoming solar radiation, to guarantee visual comfort for residents and to manage solar contributions in hot and cold seasons. To obtain the maximum potential from these technologies, it is however necessary that these devices are managed through appropriate control strategies, to compensate the currently limits of these technologies (for example, the time between the switching from one state to another) and to reach a better compromise between energy balance and luminous comfort for the occupants. The state of the art was developed around three categories, which will be briefly

described at the beginning of each paragraph: photochromic window, thermochromic window and electrochromic window.

### 2.2.1. Photochromic Windows

The literature research revealed a lack of studies evaluating the performance of photochromic (PC) windows. Photochromic materials change their transparency in response to light intensity but are not altered by temperature variation. For this reason, current research focuses on the development of hybrid PC materials and combinations of electrochromic (generally WO<sub>3</sub>-based) and photoactive films. Photochromic materials have found success in eyeglasses but are not ready for large-scale applications in building, as there are some problems such as photo response time, stability, durability, visible light coloration, reversibility, etc. [17].

An example of possible applications of the photochromic properties could be found in photochromic films for smart window applications to partially blocking the sunlight and provide visual comfort. The problem lies in the high cost and some difficulties related to production processes for large-scale applications: for this reason, Wu et al. [18] reported the development of a simpler photochromic coating (based on sol-gel matrix embedded with organic PC dyes) on glass substrate. The application of the PC films allowed the reduction of the G-value and U-value (from 0.87 and 5.2 to 0.26 and 1.58) resulting in high potential energy saving for end users especially in tropical climate.

### 2.2.2. Thermochromic Windows

Thermochromic windows are based on a temperature structural phase change, which depends on the material used. This structural change allows changes in infrared optical and electrical properties of the material. The technology may be suitable for future applications as it allows reducing the glare and solar heat gain, but currently it is still not totally ready for large-scale production, as some aspects related to high transition temperatures and low visible transmittances are not yet fully investigated [19]. The challenge is to find materials whose structural change occurs at a temperature similar to that of the room (20–25 °C), and that this change is rapid enough to adapt to the conditions required [20].

Ye et al. [21] found that during the cooling period of a year, application of VO<sub>2</sub> glazing to a residential room could save 21.7 kWh annual electricity consumption (electrical energy save near 9.4%) compared to ordinary glazing (when excluding the effect of associated lighting electricity consumption). In addition, authors have found that the cooling load could be reduced in the range of 10.2–19.9% with respect to a standard clear glazing. In the two above studies, the lighting performances were not analysed; furthermore, the application of the technology was based on the application of thermochromic VO<sub>2</sub> films on the glasses.

Yang et al. [22] simulated the heating and cooling energy consumption of three different VO<sub>2</sub> films in five typical Chinese cities; then they compared the results with white glass and Low-E glass. The dimensions of the room were 4 m × 3.3 m × 2.8 m (length × width × height) and only a single window (1.5 m × 1.5 m) was contained in the middle of the exterior wall. Results showed that cooling energy consumptions for the examined technologies could decrease by 81.7% and 70.5% compared with white glass and Low-E glass, respectively. Also in the heating period, the energy consumption of the thermochromic glass resulted to be better than Low-E glass. Anyway, all these positive results were negatively influenced by the transition temperature (that in some case was too high) and by the visual transmittance (that in some case was too low); in addition, the effect of these parameters on internal lighting was not calculated.

Costanzo et al. [23] analysed the application of TC windows in an existing office building in Italy, showing that the energy saving could range from 5% to 25%. In addition, the study considered a series of theoretical thermochromic glazing and the expected performance was compared to static clear and reflective insulating glass units. The simulations

were repeated in different climatic conditions and a detailed description of the simulation room and building was made.

In the studies previously discussed, the aspects related to the integration of windows in sample buildings were not so fully developed; in particular, those relating to the daylighting performance. In addition, experimental tests have rarely been carried out by monitoring the performance of the devices under study. As already mentioned, thermochromic glazing needs further studies especially considering the integration into the envelope and their possible impact on the energy balance of the building.

### 2.2.3. Electrochromic Window

Electrochromic glasses can regulate light penetration and transmission by responding to an electrical voltage. The main advantage is that generally they require a low voltage power source (DC 0–10 V) and that, compared to other types of smart glasses, they can be actively controlled with fast response speed and in real time, also preventing local glare phenomena within the room and solar modulation. Unfortunately, the systems are still quite expensive, and the modulation levels are still rather limited [24].

Tällberg et al., in a recent review [10], made a comparison of the energy saving potential of several window technologies. The authors found that only few studies were related to thermochromic and photochromic windows, while mostly focused on electrochromic window. With reference to the latter, most studies referred to office buildings located in different European cities.

Reynisonn et al. [25] compared three different models of windows: a traditional window without a shading, a traditional window with an external blind and a dynamic electrochromic window. They calculated that the energy saving for different locations (Kiruna, Reykjavik, Stockholm, Copenhagen, Paris, and Madrid) was between 10–30% compared to traditional window with operable blinds and 50–75% compared to a window without blinds; the authors also showed that the energy benefit was greatest for warm climates. The aspects related to internal lighting were not investigated and useful data were not obtained through experimental setup.

Ajaji and André [26] found that, for an office building in Bruxelles, the primary energy consumption could be reduced by 61% (mainly thanks to a lower cooling demand) through the use a smart electrochromic glazing. The greater assumptions were that the south face of the office was 90% glazed and that an external shading closed the opening at 50% when the solar irradiation on the window exceeded  $180 \text{ W/m}^2$  and opened when the solar irradiation dropped below  $140 \text{ W/m}^2$ .

Most of above studies did not base their analysis on experimental tests with which to compare with simulated data. Although the aspects related to day-lighting and energy performance are analysed, the studies were not always exhaustive from all points of view. In most cases, the focus concerned only one aspect (thermal, electrical, or lighting) and this was limiting, especially considering that electrochromic windows use a small part of electricity for their operation.

In conclusion, the technologies of electrochromic, photochromic and thermochromic glasses, although able to allow energy savings thanks to their characteristics and their operation, do not represent an element of the building capable of producing energy on site, differently from the STPV technology and the technology analysed in this study, the SW-LSC.

The SW-LSC technology shows the advantages of energy production without the drawbacks due to shading typical of the STPV technology, while the management of the loads is entrusted to the shading system and to the insulating characteristics of the window itself, instead of a smart glass. The innovation of this work lies in the technology analysed, which represents a meeting point between integrated solar modules and smart windows. The structure and composition of the window, equipped with a semi-transparent coloured matrix and a neutral transparent double-glazing system with a low-emissivity coating, have new optical and thermal characteristics. Moreover, starting from an experimental



setup, the study aims to propose some more general results starting from the use of a calibrated energy model.

### 3. Materials and Methods

The methodology used in this study involves different types of analysis: environmental, daylighting, thermo-physical, and electrical performance investigation. The starting point was the experimental study, which made it possible to obtain data relating to the characteristics of the LSC and traditional windows, installed in an office in Eni Research Center, in the city of Novara. Furthermore, the data relating to the generation and the electricity consumption (due to the movement of the venetian blinds) related to two years of monitoring were collected and reprocessed. Subsequently, an experimental setup was prepared to conduct the lighting tests, which allowed the validation of the models created in a test room and then the simulation of the same models on a larger-scale building model.

The methodology can be summarized in the following steps:

- Assessment of environmental aspects related to the smart window through the Life Cycle Assessment (LCA) methodology;
- Development of monitoring studies that concerned the monitoring of generation and consumption of LSC modules through a computer and a sensor placed outside the SW-LSC, the monitoring of daylight inside the two rooms where the SW-LSC and the traditional window were installed, the meteorological and climatic monitoring through a weather station on the roof of the building. The monitoring of the electrical performances relating to the SW-LSC made it possible to obtain the generation and consumption of the device. The analysis covered about two years of monitoring, from 30 April 2017 to 18 November 2019, accounting for the experimental data acquired in the framework of the R&D project dedicated to the development of the Smart Window and prototype validation in real operating conditions. The daylighting analysis regarded a series of measurement of illuminance level (lux) in different points of the rooms. The monitoring study was carried out through a lux meter and a weather station located outside the building that simultaneously recorded the weather data. The two window models were tested on a sample room, which had the same characteristics (size and internal structure) as the real one. After the simulation, the results of the simulations were compared with those of the measurements and the percentage error between the two values (simulated and measured) was calculated. Finally, authors focused on the uncertainties of the model parameters, through a calibration process.

The SW-LSC and the traditional window models were created. Both models were developed to reproduce optical, geometric, and thermal characteristics of the two windows.

- The thermo-physical analysis based on the windows models previously created. In this step, authors evaluated the thermo-physics aspect on the SW-LSC compared to those of the traditional window. In this case, the window models were tested on a large-building model.
- The electrical performance analysis started with a simple regression approach to evaluate the relationship between power output from LSC modules and incident solar radiation. Then, the model was used to obtain the generation of the SW-LSC device in a large-building simulation.

The methodology steps are showed in Figure 1.

#### 3.1. Experimental Setup

The SW-LSC prototype was installed in a test room where the input and output data from the device were monitored and the control logic of the same was managed via a computer. For our case study, the room was an office. The room was 3 m × 4 m × 3.5 m (L × W × H) wide and was placed on the second floor of a building in Novara (latitude 45.45°, longitude 8.64°, altitude 156 m). The traditional window was installed in the room

corresponding to the first floor. As this second room was open on one side (for the presence of a stairwell), it was closed and made of the same size as the test room through a thick curtain that simulates a clear white wall (Figure 2). This step was necessary to validate correctly the model based on the lighting measurements made into the rooms.

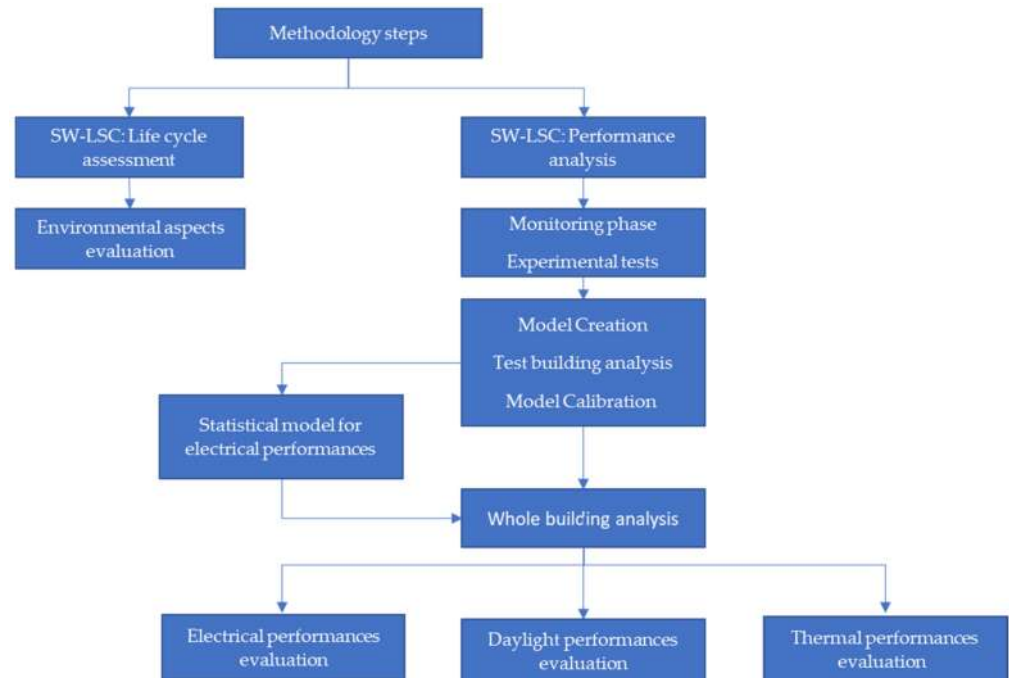


Figure 1. Graphical illustration of the analysis steps.



Figure 2. The curtain used to reproduce the white wall (different views).

Both windows faced south-east, with an azimuth of  $27^\circ$  and there were no obstacles due to other building or other obstructions in front of the windows. The structure of the walls involves the use (from outside to inside) of natural stone (travertine), mortar, brick, and a layer of plaster. The walls and ceiling are characterized by a clear white colour, while the floor by a smoke grey colour, due to the rubberized carpet pad.

The SW-LSC integrated system is an innovative multifunctional window model, integrated by luminescent solar concentrators designed to generate electricity. The window is designed to offer advanced energy performance, while guaranteeing its own energy self-sufficiency for the purpose of the operation of automatic solar control systems (automated venetian blind).

The SW-LSC device had two distinct parts: in the upper part of the window, four semi-transparent yellow LSC modules were integrated into an aluminium mask, while in the lower part, there was a double-glazing window. The lower section, subsequently called “window”, had two opening window sashes, while the upper one, called “transom

window”, was based on semi-transparent LSC modules [27]. The “colour” of the LSC modules was static and was mainly due to the electrical operation of the same; it also had a beneficial effect on the internal light of the environment [28]. A venetian blinds system, connected to an irradiation sensor located outside the window and to a control logic system, managed the control of the internal load. The venetian blinds system was motorized and the LSC modules in the upper part produced the necessary energy for his functioning: the energy was sufficient to move the shading system even on cloudy days and for relative long periods (5 days), thanks to a storage batteries system [29]. Between the two sections of the SW-LSC there was a light shelf (a reflecting shelf), positioned between the smart window and LSC modules. This component intercepts part of the incident solar radiation and diffuses it into the internal environment with greater depth and uniformity, while ensuring shading near the window and reduced glare; it was 0.4 m large and 2.342 m wide [30].

In detail, the device was made with thermal break aluminium profiles ( $U_f = 1.9 \text{ W/m}^2 \text{ K}$ ), while the coloured semi-transparent (yellow) modules were four LSC slabs, each  $50 \times 50 \text{ cm}$ . The dimensions of the SW-LSC were  $2.285 \text{ m} \times 2.344 \text{ m}$  (L X W) and the layout of the device is shown in Figure 3 [31].

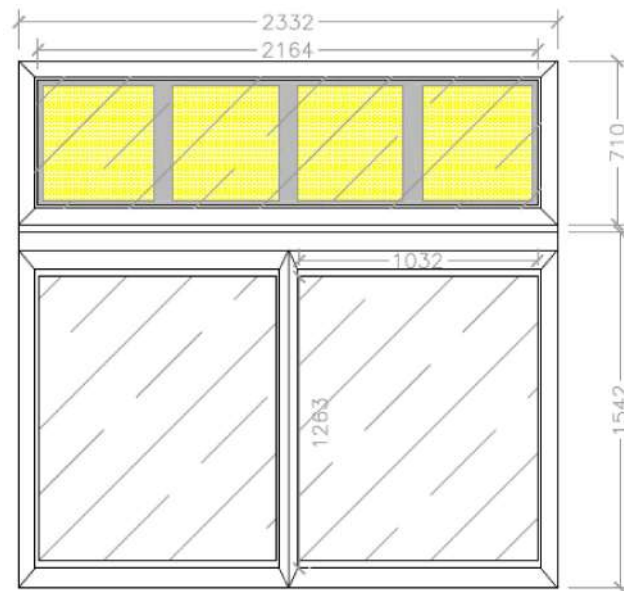


**Figure 3.** Sketch of the SW-LSC system.

In detail, the layering of the upper double-glazing (transom window) with U-value of  $1.2 \text{ W/m}^2 \text{ K}$  are shown in Figure 4.

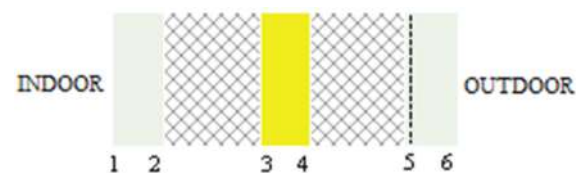


**Figure 4.** Stratigraphy of the upper double-glazing (transom window) with the LSC technology integrated. 1–2, an extra-clear laminated glass of 6.76 mm on the outside; 2–3, a gap of dehydrated air, 12 mm; 3–4, the central element is a (yellow) PMMA slab that incorporates the ENI REI plus technology, 6 mm thick; 4–5, a gap of dehydrated air, 12 mm; 5–6, an extra clear low emissive laminated glass, 6.76 mm thick, with the low emissive layer applied in face 5, as internal glass.

The total thickness of the double-glazing was 49.52 mm.



Each window sash of the lower part of the window is made of double extra clear glass filled with air with a 4 + 4.2/22/4 + 4.2 stratification ( $U_g = 1.1 \text{ W/m}^2 \text{ K}$ ). The internal glass was covered with a low emissive layer applied in face 3, as shown in Figure 5.

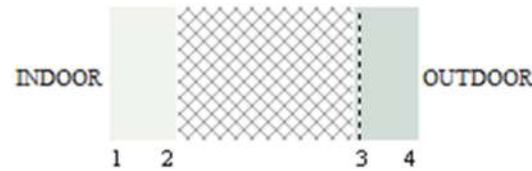


**Figure 5.** Stratigraphy of the lower double-glazing.

The upper and lower part of the window were divided by a horizontal aluminium shelf, which extended from the inside to the outside of the building. The shelf helped to mix the coloured light that passes through the LSC panels with the clear light that passes through the neutral glass below, to obtain a natural light characterized by a lower colour temperature [32,33]. In addition, it should have allowed reducing direct radiation inside the room, avoiding unpleasant glare inside the room.

The window models have the characteristics shown in Table 1.

**Table 1.** Thermo-optical characteristics of the SW-LSC and of the traditional window.

Name	SHGC	Solar Transmittance at Normal Incidence	Visible Transmittance at Normal Incidence
SW-LSC (upper window)	0.49	0.409	0.678
SW-LSC (lower window)	0.507	0.383	0.631
Traditional window	0.819	0.775	0.881

The window sashes integrated double-glazing with high thermal resistance glass, equipped with an automated solar control system made with venetian blinds placed in the cavity. The movement of each slat was controlled by an electric motor, integrated in the double-glazing itself. The engine was powered by a high efficiency battery, which was charged by the electricity generated by the LSC modules. A solar irradiation sensor was placed at about 1/4 of the height of the upright of the window frame starting from the sill and it is shown in Figure 6 [34].

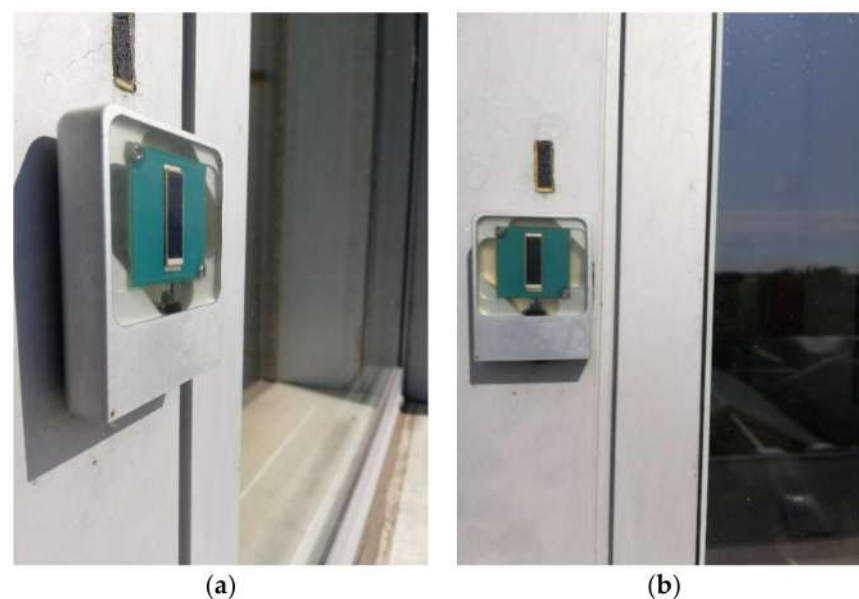


**Figure 6.** (a) The solar irradiation sensor placed on the external side of the window. (b) Position of the solar radiation sensor.

The control logic system, connected to the external solar radiation sensor, adjusts the opening level of the slats. The irradiation sensor was a monocrystalline silicon photovoltaic cell, type IXYS KXOB22, with voltage and current values in STC equal to 0.5 V and 44.6 mA, respectively [35]. The system detected the level of solar irradiance on the external surface of the window and, when the measured value exceeded a certain threshold ( $180 \text{ W/m}^2$ ), the solar shading system was activated by lowering the blinds in order to completely shield the direct incident solar radiation (Figure 7a). When the irradiance value was reduced below the set threshold the blinds were completely opened (Figure 7b). The system provided the possibility for the user to redefine the irradiance threshold that controls the closing/opening of the slats [36,37].



**Figure 7.** (a) Shading system in the configuration of the window completely closed. (b) Shading system in the configuration of the window completely opened.

The traditional window was a single glass panel (5 mm glass,  $U_g = 5.6 \text{ W/m}^2 \text{ K}$ ) with an aluminium frame and roller shutters as shading device. The window had the same dimension of the SW-LSC but due to the different configuration, it had a higher glassed area. The traditional window is shown in Figure 8.



**Figure 8.** The traditional window located on first floor.

A weather station placed on the roof of the building, monitored the following data with a timestep of one second:

- External Temperature;
- Global solar radiation;
- Diffuse solar radiation;
- Direct solar radiation;
- Wind speed;
- Wind direction;
- Atmospheric pressure.

### 3.2. Environmental Aspects of SW-LSC and LCA

Before the experimental tests and the analysis of the SW-LSC performances, a LCA of the prototype was conducted [38]. The SW-LSC prototype was analysed in its entirety, considering the shading system (venetian blind system), the light shelf and the accessory components (batteries, motors, sensor, etc.) that allow the device to function.

The functional unit was the whole SW-LSC (5.27 m<sup>2</sup>) considering its thermal and optical characteristics ( $U_w = 1.6\text{--}1.8 \text{ W/m}^2\text{K}$ ,  $t_{vis} = 77\%$  and  $g = 85\%$  of LSC modules). The analysis followed a cradle to gate approach. The results of the analysis are showed in Table 2.

**Table 2.** Environmental impacts of SW-LSC.

Impact Categories	Unit	Production	Assembly
Abiotic depletion potential	kg Sb eq	$3.0 \times 10^{-2}$	$3.0 \times 10^{-7}$
Abiotic depletion potential (fossil fuels)	MJ	$5.4 \times 10^4$	3.6
Global warming potential	kg CO <sub>2</sub> eq	$5.7 \times 10^3$	$4.0 \times 10^{-1}$
Ozone layer depletion potential	kg CFC <sub>11</sub> eq	$2.1 \times 10^{-4}$	$1.6 \times 10^{-8}$
Human toxicity	kg 1,4-DB eq	$5.3 \times 10^3$	$3.5 \times 10^{-1}$
Fresh water aquatic ecotox.	kg 1,4-DB eq	$3.6 \times 10^3$	$2.2 \times 10^{-1}$
Marine aquatic ecotoxicity	kg 1,4-DB eq	$4.7 \times 10^7$	$3.3 \times 10^3$
Terrestrial ecotoxicity	kg 1,4-DB eq	$1.2 \times 10$	$1.4 \times 10^{-3}$
Photochemical oxidation	kg C <sub>2</sub> H <sub>4</sub> eq	2.00	$1.4 \times 10^{-4}$
Acidification potential	kg SO <sub>2</sub> eq	$3.2 \times 10$	$2.3 \times 10^{-3}$
Eutrophication potential	kg PO <sub>4</sub> eq	8.3	$5.6 \times 10^{-4}$

Considering only the production phase, the SW-LSC components contribution to the impact categories is shown in Figure 9.

The most impactful components of the SW-LSC system were the window frame (environmental impact was above 60% in all categories, except for abiotic depletion, where the contribution was 16.22%), the light shelf (from 16.29% to 25.02% except abiotic depletion where the contribution was only 2%), and the DC motors and batteries (30.74% and 36.26%, respectively, in abiotic depletion but a low contribution (less than 4%) in all other categories). The LSC modules contributed less than 5% in all impact categories.

From an environmental point of view, the prototype can be further improved, and the design could allow the use of other less energy-intensive materials. For the same reason, the substitution, or the remotion, of potentially “onerous” elements from an environmental point of view, such as the light-shelf, could be evaluated.

In conclusion, the LCA of the SW-LSC prototype allowed to quantify the environmental burdens of the device and to highlight the critical elements of the system. Although further studies regarding this technology are required, especially considering large-scale production processes and the consequent use of raw materials with greater efficiency, the device represents a promising alternative to exploit a different type of installation into building in urban contexts.

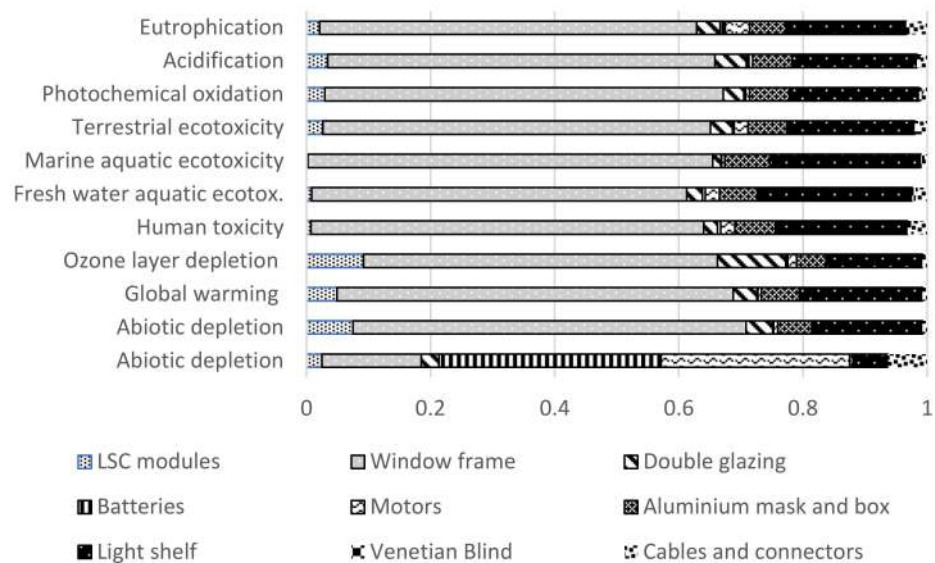


**Figure 9.** Contribution of the SW-LSC elements.

### 3.3. Experimental Tests

To validate the SW-LSC lighting model, data collection studies were carried out through the measurement of illuminance levels (lux) in different points of the room where the SW-LSC prototype was installed (Figure 10a). At the same time, the measurements were also carried out in the room located on the first floor of the same building, as for the test room, which had the same dimensions but was equipped with a traditional window (Figure 10b).

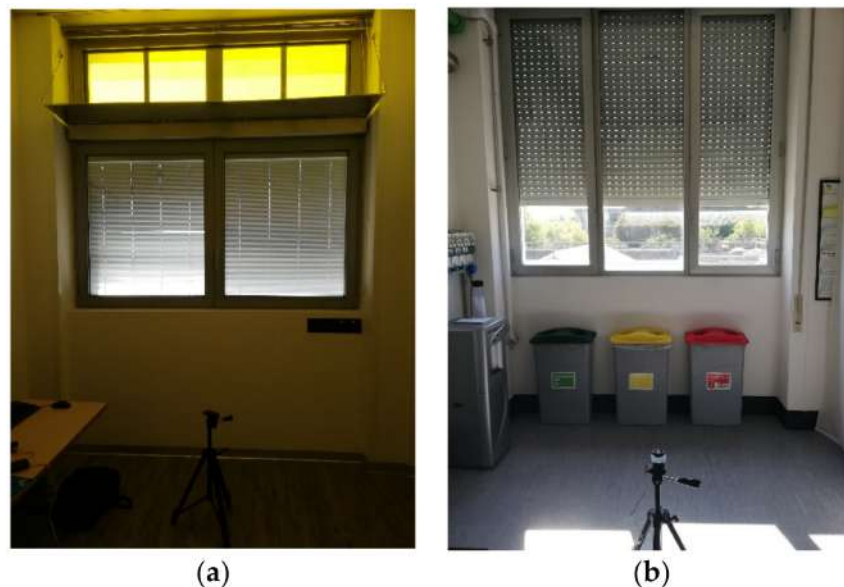


**Figure 10.** (a) Inside view of second floor room (SW-LSC), (b) Inside view of first floor room (traditional window).

The monitoring studies were conducted using a lux meter, which is the instrument generally used for measuring illuminance and light intensity in environments and workplaces. The measurements were conducted in five points in both rooms at a height of 0.8 m, the height recommended by the regulations UNI EN 12464-1 for the workplace; the map of the test room and the position of the five points are shown in the Figure 11.

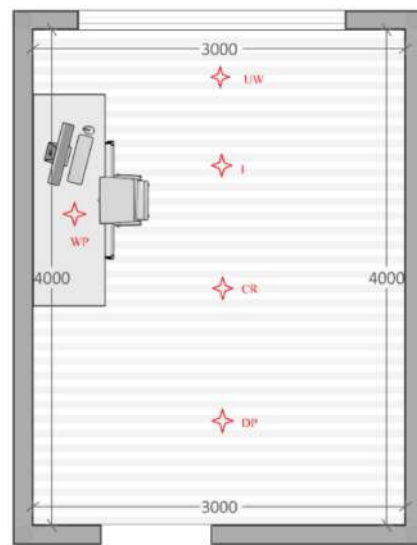


**Figure 11.** Location of measuring points inside the room.

The points were named as follow:

- Under window (UW) with coordinates:  $x = 1.5$ ;  $y = 0.5$ ;
- Work plan (WP) with coordinates:  $x = 0.8$ ;  $y = 1.5$ ;
- Intermediate (I) with coordinates:  $x = 1.5$ ;  $y = 1$ ;
- Centre of the room (CR) with coordinates:  $x = 1.5$ ;  $y = 2$ ;
- Door proximity (DP) with coordinates:  $x = 1.5$ ;  $y = 3$ .

The measurements were carried out on 18 February 2020 from 11 a.m. to 4 p.m. at half hour intervals for both rooms with the shading devices deactivated; in the case of the SW-LSC, the venetian blinds were positioned in the “fully open” mode and the same was done with the shutters of the traditional window. The day chosen was completely sunny, to prevent the passage of clouds from affecting the measurements. The artificial lights were switched off during the whole duration of the measurements. The only internal load inside the rooms was the computer (250 W) that monitored the performance of the SW-LSC and regulated the shading system.

The monitoring data relating to the electrical performance of the SW-LSC referred to two years of monitoring. The data were based on the generation of electricity, the accumulation of energy in the batteries and the consumption of the motors, recorded with a timestep of one second. The data re-processing made it possible to account for the daylight savings period (aligning the times with the monitoring ones), the accidentally consumption due to a movement of the blinds activated manually (and not through the threshold set by the control system), for system maintenance and lockouts and, finally, to aggregate the same as daily production and consumption. The re-elaboration was carried out by exploiting the recorded climatic data concerning the external temperature and radiation on the vertical surface of the window.

### 3.4. Modelling

#### 3.4.1. Daylighting Performances

The modelling of the two windows (frames and structure) was performed in Energy plus environment. The structure of the glass, of both the traditional windows and of the SW-LSC, was built using Window\_7 software that allowed creating and managing more complex stratigraphy and layers such as that of the upper window. This model was subsequently uploaded to EnergyPlus and Open studio environment.

The assumptions on the modelling were that heat exchanges occur only through the south facade, while the other surfaces were adiabatic. The materials used for the walls were those listed in the previous section (Section 3.1). The office room was set to be occupied



by one person from 7:00 a.m. until 6:00 p.m. during working days, with a break for lunch from 00:00 p.m. to 1:00 p.m. The other parameters were set to match what was prepared during the experimental setup.

Two models were created, one per each room. The windows had the same dimensions, but due to the different layout, the glazed surface of the traditional window was slightly greater. The model had a single room and a single thermal zone and is shown in Figure 12.

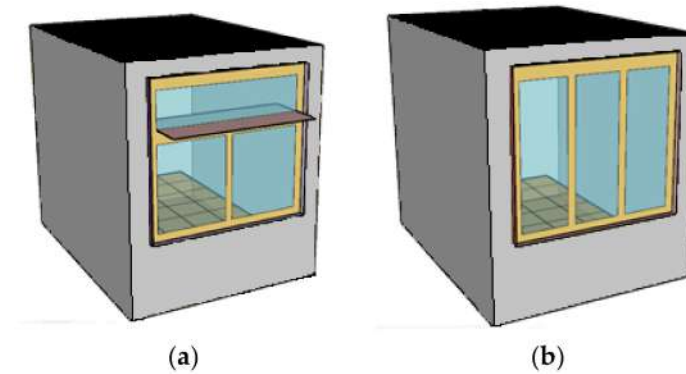


**Figure 12.** (a) Room model with the SW-LSC, (b) Room model with the traditional window.

The data output from the weather station described in the previous paragraph was implemented into a weather data file imported into the building simulation tool used.

Subsequently, these data were re-elaborated to obtain these variables with a one-minute timestep, to be consistent with the monitored data.

The simulation was run with one-minute timesteps.

The calibration process was performed for the optical properties of the internal walls, of the outside obstructions and of the light shelf. The other important element was the light shelf, present only in the configuration of SW-LSC. A high reflectance layer covered this aluminium element, and it was necessary to proceed by attempts to correctly simulate the characteristics and functioning of the element. Due to the limited measurement range of the luxmeter used, especially for high illuminance values, and due to some localized shading due to the structure of the windows, an error of 10% with respect to the monitored data was considered acceptable.

### 3.4.2. Energy Generation Statistical Modelling

Due to the limited availability in the physical generation models for the technology investigated a simple regression model was used to investigate the relationship between power output from LSC modules and incident solar radiation. A regression model is a statistical linear model that, in case of more input variables, can be expressed as Equation (1):

$$y = \beta_0 + \beta_1 x_1 + \beta_2 x_2 + \dots + \beta_r x_r + \varepsilon \quad (1)$$

In which:

- $y$  is the real output
- $\beta_0, \beta_1, \beta_2, \dots, \beta_r$  are the regression coefficients
- $x_1, x_2, \dots, x_r$  are the independent variables
- $\varepsilon$  is the random error

In case of  $r = 1$ , the model become a simple linear regression one (Equation (2)):

$$y = \beta_0 + \beta_1 x_1 + \varepsilon \quad (2)$$

where  $\beta_0$  is also called intercept. Estimation of regression coefficients  $\beta_0$  and  $\beta_1$  is usually done through the Least Squares method, that aim to minimize the error between predicted

and real targets. The function to minimize, denoted as SS function, can be expressed in the following way (Equation (3)):

$$SS(\beta_0, \beta_1) = \sum_{i=1}^n (y_i - \hat{y}_i)^2 = \sum_{i=1}^n (y_i - \beta_0 + \beta_1 x_i)^2 \quad (3)$$

In order to minimize SS function, it is compulsory to find two estimators, the so-called least-square estimators and denoted as  $\hat{\beta}_0, \hat{\beta}_1$ . This is done deriving function SS with respect to the estimators and putting the results equal to zero (Equation (4)):

$$\begin{cases} \frac{dSS}{d\hat{\beta}_0} = -2 \sum_{i=1}^n (y_i - \hat{\beta}_0 + \hat{\beta}_1 x_i) = 0 \\ \frac{dSS}{d\hat{\beta}_1} = -2 \sum_{i=1}^n (y_i - \hat{\beta}_0 + \hat{\beta}_1 x_i) x_i = 0 \end{cases} \quad (4)$$

Results for  $\hat{\beta}_0$  and  $\hat{\beta}_1$  are obtained introducing new variables  $\bar{y}$  and  $\bar{x}$ , and solving latter Equations (5) and (6):

$$\hat{\beta}_0 = \bar{y} - \hat{\beta}_1 \bar{x} \quad (5)$$

$$\hat{\beta}_1 = \frac{\sum_{i=1}^n (x_i y_i) - \bar{x} \sum_{i=1}^n y_i}{\sum_{i=1}^n (x_i)^2 - n \bar{x}^2} \quad (6)$$

In which  $\bar{y}$  and  $\bar{x}$  are expressed in the following way (Equations (7) and (8)):

$$\bar{y} = \frac{1}{n} \sum_{i=1}^n y_i \quad (7)$$

$$\bar{x} = \frac{1}{n} \sum_{i=1}^n x_i \quad (8)$$

The simple linear regression can be expressed as Equation (9):

$$\hat{y} = \hat{\beta}_0 + \hat{\beta}_1 x_1 \quad (9)$$

Variable  $\hat{y}$  represents model output in Equation (9).

Assessment of the model can be done using model performance metrics, such as the coefficient of determination  $R^2$ , the root mean square error RMSE and the mean bias error MBE. The former one represents the goodness of fit of the model and can be expressed in the following way (Equation (10)):

$$R^2 = 1 - \frac{SS}{SS_{total}} = 1 - \frac{\sum_{i=1}^n (y_i - \hat{y}_i)^2}{\sum_{i=1}^n (y_i - \bar{y})^2} \quad (10)$$

where SS is the residual sum of squares and  $SS_{total}$  is the total sum of squares. In other words, R-square relates variance explained by the model with respect to the total variance. It ranges within the interval [0,1], assuming value equal to 1 in case of perfect fit of data. The RMSE, instead, represents standard deviations of the residuals and it is used to evaluate accuracy of the model itself. The lower is the RMSE value, the better the accuracy. In mathematical terms (Equation (11)):

$$RMSE = \sqrt{\frac{1}{n} \sum_{i=1}^n (y_i - \hat{y}_i)^2} \quad (11)$$

Finally, MBE represents the average distance between predicted and real targets (Equation (12)):

$$MBE = \frac{1}{n} \sum_{i=1}^n (y_i - \hat{y}_i) \quad (12)$$

### 3.4.3. Building Performance Simulation

After the experimental system was characterized and calibrated, the models created were tested on a larger building, to evaluate the thermal performances of the system in a real building environment.

The small office model proposed by ASHRAE Standard 2019 was a building with a floor area of 511 m<sup>2</sup>; the building plan and the perspective view of the building are shown in Figure 13. The building was composed of one attic and five thermal zones; among these five thermal zones there was a central area that had no external walls and four perimeter areas which were each exposed towards a respective direction (north, south, west, east). The perimeter areas were the only ones equipped with window surfaces (four windows for west and east surface, six windows for south and north surfaces).

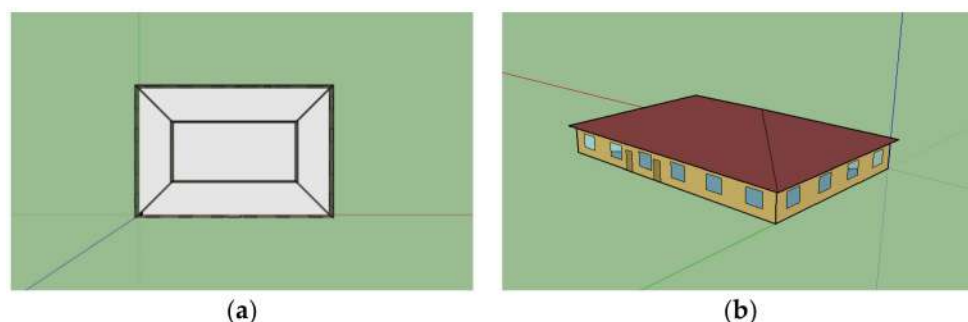


**Figure 13.** Plan (a) and perspective (b) view of the small office.

For the analysis carried out, the windows of the reference model were entirely replaced, in the first model, by the traditional window (traditional window scenario) and, in the second model, by the SWs-LSC (SW-LSC scenario), keeping the original dimensions for both.

The authors chose four days that had particular characteristics of irradiation and temperature and that were, therefore, representative of the most critical periods and seasons from a thermal point of view, as described in other literature [39,40]. These days were:

- Cold cloudy (24 December);
- Cold sunny (15 January);
- Warm cloudy (28 August);
- Warm sunny (22 July).

The choice of the days was made using the hourly climate data for the city of Novara.

Table 3 shows the outdoor dry-bulb temperature (Dbt) and the global horizontal radiation (GlobHorRad) for the four selected days. Moreover, as seen in Table 2, the chosen days were significant for the differences or similarities to the average monthly values.

**Table 3.** Reference days characteristics.

Reference Days	Mean Dbt °C	Mean GlobHorRad Wh/m <sup>2</sup>	Month	Mean Dbt °C	Mean GlobHorRad Wh/m <sup>2</sup>
24 December (cold cloudy)	−1.8	68.2	December	2.8	118.3
15 January (cold sunny)	−4.5	136.2	January	1.7	136.2
22 July (warm sunny)	27.2	550.5	July	23.6	429.3
28 August (warm cloudy)	24.8	219.8	August	22.9	349.4

## 4. Results

### 4.1. Monitoring

The day-lighting monitoring study performed with a lux-meter made it possible to obtain the level of illumination in different points of the two rooms where the SW-LSC and the traditional windows were installed.

The results of the monitoring are shown in Tables 4 and 5.

**Table 4.** Illuminance values recorded during the monitoring study for and traditional window.

Traditional Window—Monitoring Results [Lux]					
Time	Points				
	UW	I	CR	DP	WP
11:00	6900	26,600	22,400	22,200	36,300
12:00	6720	9700	50,700	48,200	61,700
13:00	7530	55,000	7050	4530	55,500
14:00	6220	6690	4620	2640	7900
15:00	4390	4420	2930	1930	3720
16:00	1650	1710	1160	800	1700

**Table 5.** Illuminance values recorded during the monitoring study for SW-LSC.

SW-LSC—Monitoring Results [Lux]					
Time	Points				
	UW	I	CR	DP	WP
11:00	3500	4300	3740	3400	19,800
12:00	3520	46,800	46,660	3560	44,800
13:00	3350	47,100	3240	2340	40,600
14:00	3060	3300	2320	1760	2750
15:00	2220	2500	1730	1270	1850
16:00	910	1107	825	630	864

Results show that for the UW point, the presence of the light shelf allows the reduction of excessive illuminance on the work plane. In general, in the case of the SW-LSC, the mix between the yellow light that filters from the LSC modules and that of the lower part window as well as the presence of light shelf, allowed lower values of the illuminance in most points in the room.

The analysis of the electrical data relating to the SW-LSC made it possible to obtain the generation and consumption of the device. The analysis covered about two years of monitoring, from 1 June 2017 to 18 November 2019. During this period, the average monthly energy generated by LSC modules in SW-LSC was around 7.1 Wh (2017), 6.8 Wh (2018), 5.9 Wh (2019); the monthly energy absorbed by electric motors was 0.8 Wh (2017), 0.9 Wh (2018) and 1.1 Wh (2019).

The data analysed were from 2018, which was the only complete year. The net electricity generation for 2018 was approximately 1.5 kWh, with an average daily production of 5 Wh/day.

The annual consumption was about 0.27 kWh, due to the movement of venetian blinds system and in rare cases, to the recharging of small devices connected via USB at the output of the production system. In some periods of high production, the non-consumed energy that exceeded the capacity of the batteries was released on a resistor.

The highest average monthly production was recorded in September (8.9 Wh) while the lowest (2.4 Wh) in November as shown in Figure 14. An example of the trend of daily generated and adsorbed energy is showed in Figures 15 and 16.

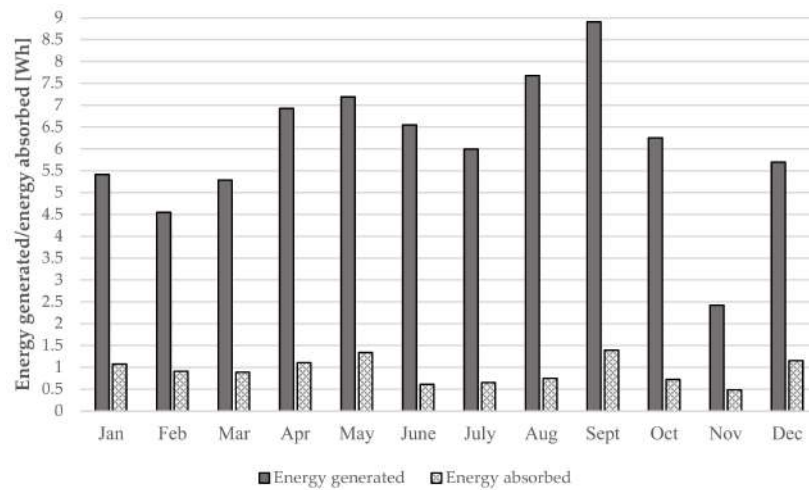


Figure 14. Monthly energy generated and absorbed for year 2018.

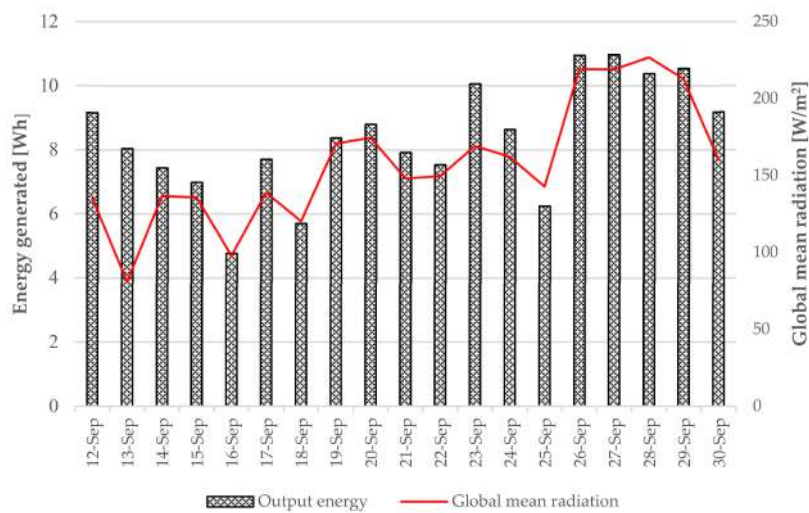


Figure 15. Daily energy generated during the period 12–30 September 2018.

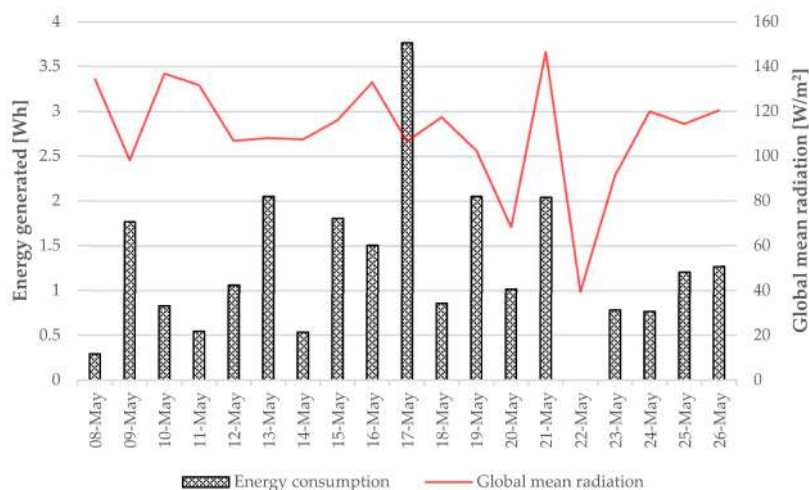


Figure 16. Daily energy absorbed during the period 8–26 May 2018 reported with global mean radiation.



It should be noted that consumption was strictly linked to the threshold set for the activation of the shadowing system and the climatic conditions. In fact, on some days of partial cloud, it happened that the activation of the shading system occurred frequently due to oscillations above and below the threshold value, causing a higher consumption than normal.

4.2. Daylighting Model Calibration

The models of the traditional window and the SW-LSC were used inside the test building; the simulations using the illuminance map allowed to obtain the illuminance value at the points of the experimental test. The comparison between the simulated and monitored values after the calibration process in the test room is shown in Figures 17 and 18:

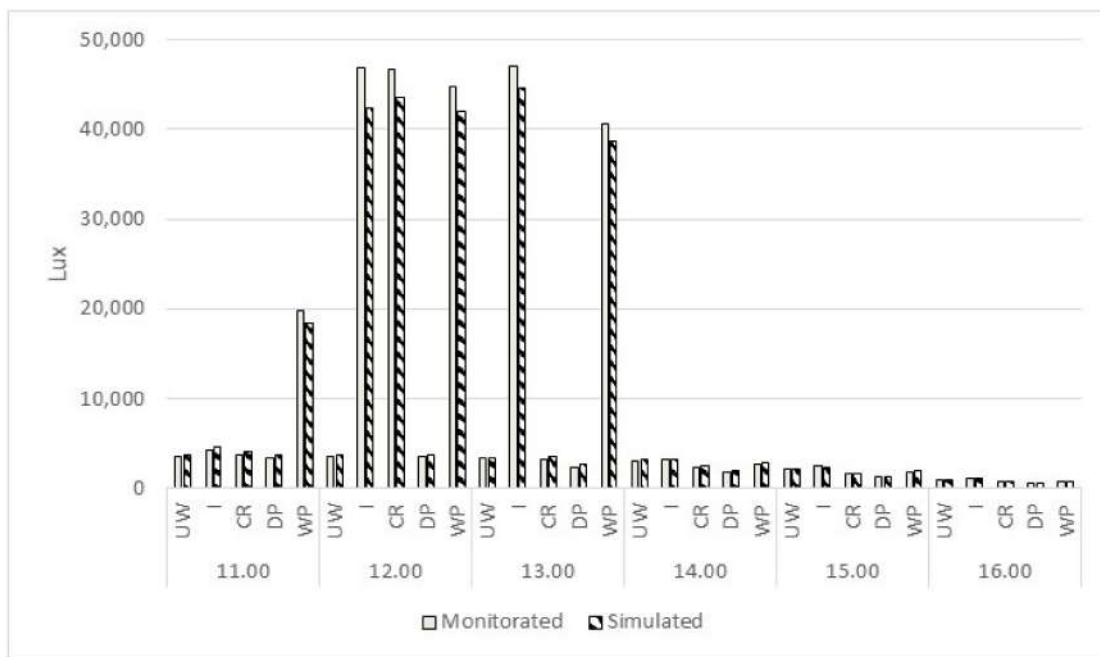


Figure 17. Gap between monitored and simulated value [lux] for SW-LSC model.

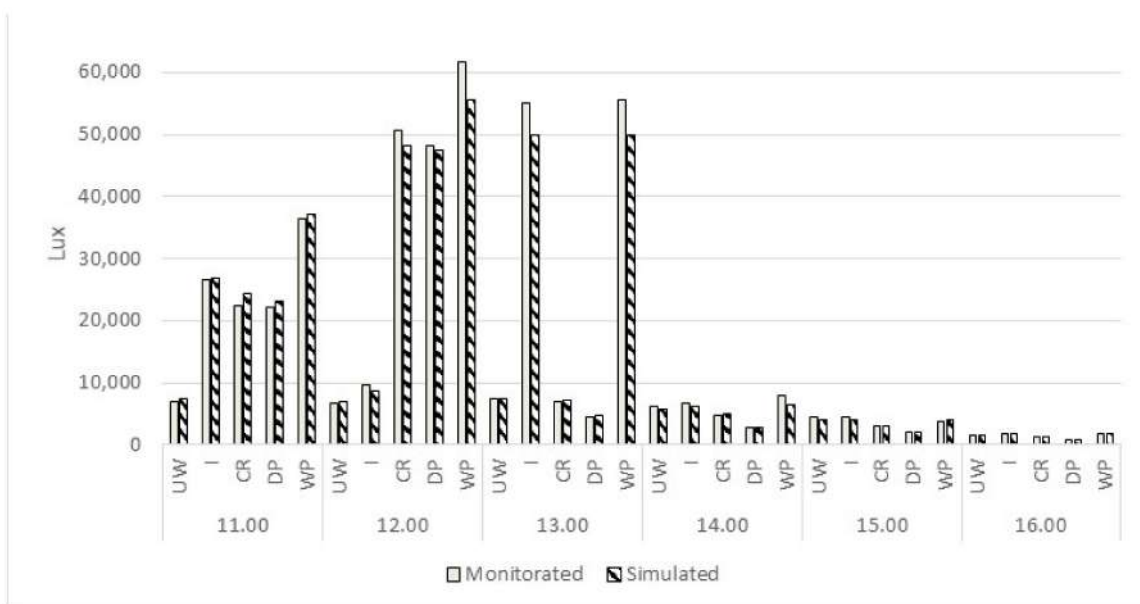


Figure 18. Gap between monitored and simulated value [lux] for traditional window model.

To evaluate the accuracy of the models, the percentage error between the measured and the simulated value was calculated; the percentage error was expressed as the absolute value of the difference between the measured and estimated value, divided by the absolute value of the value measured, multiplied by 100. Most of the percentage errors calculated were around or below 10%.

In the case of SW-LSC, the error for I point at 12:00 and 13:00, CR at 12:00 and WP at 12:00 was higher than 10% (around 25%) due to irradiation values that were too high for the range of the measuring instrument used. For the same reason, in the case of traditional window, WP at 12:00 showed a higher error (22,5%). The DP at 14:00, 15:00 and 16:00 showed a high error (46%, 32% and 36%, respectively), as well as WP at 14:00 due to localized shading at the measuring point during the monitoring phase.

In conclusion, however, the models were a good approximation of reality and were validated for the cases of the traditional window and the SW-LSC. The calibrated models will be used in the whole building analysis.

#### 4.3. Energy Generation Regression Analysis

As mentioned in the previous paragraph, a statistical analysis between electrical power produced by the LSC modules and incident solar radiation was performed. A stochastic model is usually used when there is a lack of information regarding physics involved within natural phenomena under study. Raw data for three variables were provided by sensors installed near LSC modules. Particularly, data on electricity produced, incident solar radiation on the modules and cell temperature were collected from 30 April 2017 to 18 November 2019, with a sub-minutely time-step (each measurement was performed every 30 s). Daily time range of observations were made from 7 a.m. to 7 pm. Firstly, anomalies were detected and removed. Then, the raw data were aggregated into hourly values, the averaging through the arithmetic mean.

Hourly mean values were normalized in the interval [0,1], applying min-max scaling method (Equation (13)):

$$z(x) = \frac{(x - \min(x))}{(\max(x) - \min(x))} \quad (13)$$

where  $z$  represent the normalized hourly variables. A further step was to split data into two groups, one for training the regression model, the other for the testing it. Within the former cluster, 2017 and 2018 data were included, whereas instead the testing sample included 2019 data. Figure 19 shows two graphs, the first shows the trend of normalized solar generation with respect to normalized solar radiation, the latter with respect to cell temperature. The correlation between the LSC power output and solar radiation can be clearly seen. In contrast, cell temperature has a null or weak correlation with the component generation. As that regression analysis was conducted exploiting only solar radiation as an independent variable, a simple regression linear model was analysed to explore a possible correlation between the above-mentioned variables (Figure 20), (Table 6). Mathematical details of the model were formulated in the previous paragraph. The analysis was conducted in the MATLAB environment and a bisquare robust option exploited, that is less sensitive to anomalous values, allowing the analyst to not remove manually outliers. In Figure 21, the real and fitted data are reported for two datasets used within the analysis.

**Table 6.** Main features of the regression model.

	Regression Model	R <sup>2</sup>	RMSE	MBE
Training set (2017–2018)	$Y = 0.7077 \times x + 6.024 \times 10^{-6} + \varepsilon$	≈0.95	≈0.04	≈0.02
Testing set (2019)		≈0.87	≈0.07	≈0.01

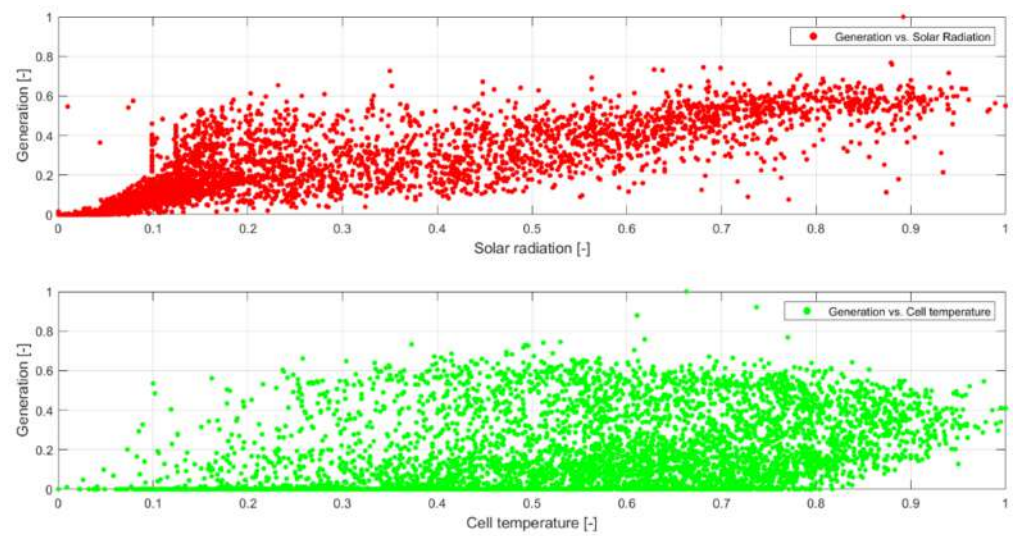


Figure 19. LSC energy generation vs. other variables.

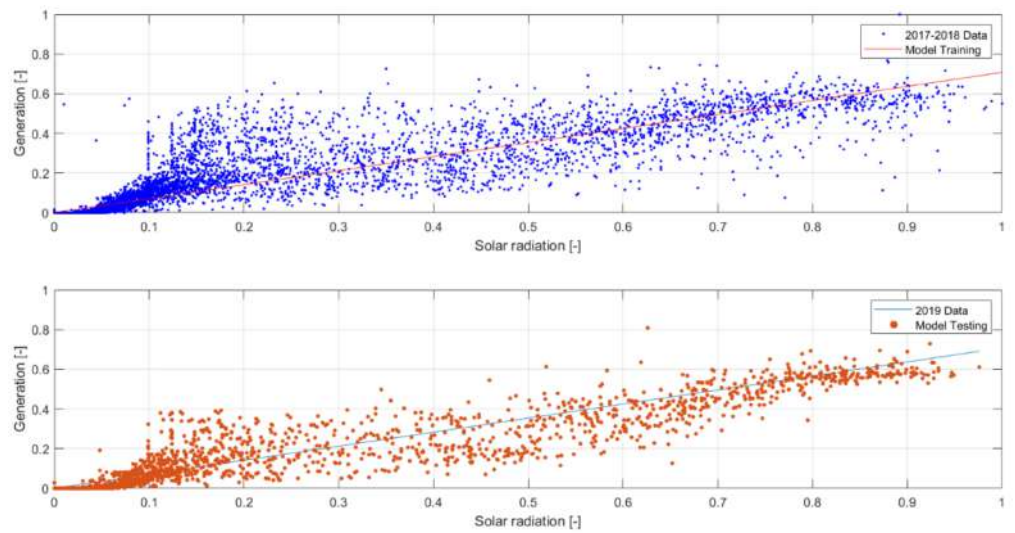


Figure 20. Linear robust fitting for training and testing data.

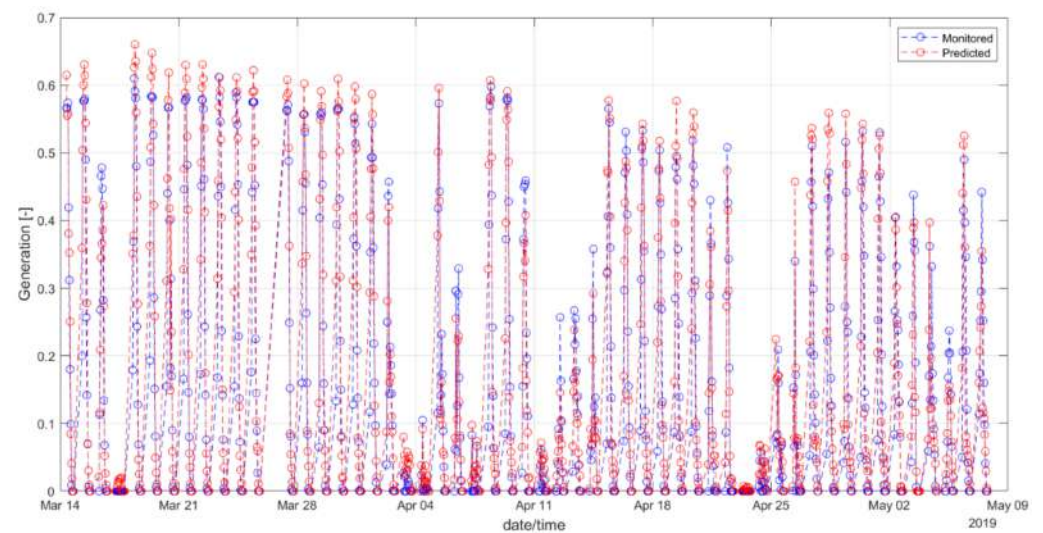


Figure 21. Real vs. predicted LSC energy production values for a selected period.

#### 4.4. Whole Building Analysis

##### 4.4.1. Daylight Analysis

For the daylight analysis of the entire building, the annual calculation of the Daylight Autonomy (DA) is proposed to quantify the annual daylight and to determine the level of direct sunlight both in the case of the SW-LSC and the traditional window. The DA value is defined as the percentage of time in a year that daylight can provide a given illuminance for a chosen point.

The method used (incremental method) assumes that the illuminance of daylight must exceed the illuminance required for the given time. In this study, we chose to analyse the DA for two values: a minimum threshold value of 300 lux and a maximum value of 500 lux, which is the recommended one for normal office work and PC work. The analysis period was a full year, and we assumed the occupied hours to be standard office work hours from 8 a.m. to 6 p.m. and 9 a.m. to 5 p.m., depending on the season. An acceptable value of DA was set at 50%, i.e., if the set threshold of illuminance was reached for at least 50% of the hours during the year.

The illuminance maps were created for all four perimeter areas of the building (facing north, southwest, and east) excluding the central area and the attic, which were not equipped with windows and were not exposed to direct solar radiation. The illuminance maps cover most of the area useful for office work, excluding the perimeter areas of the rooms, as shown in Figure 22.

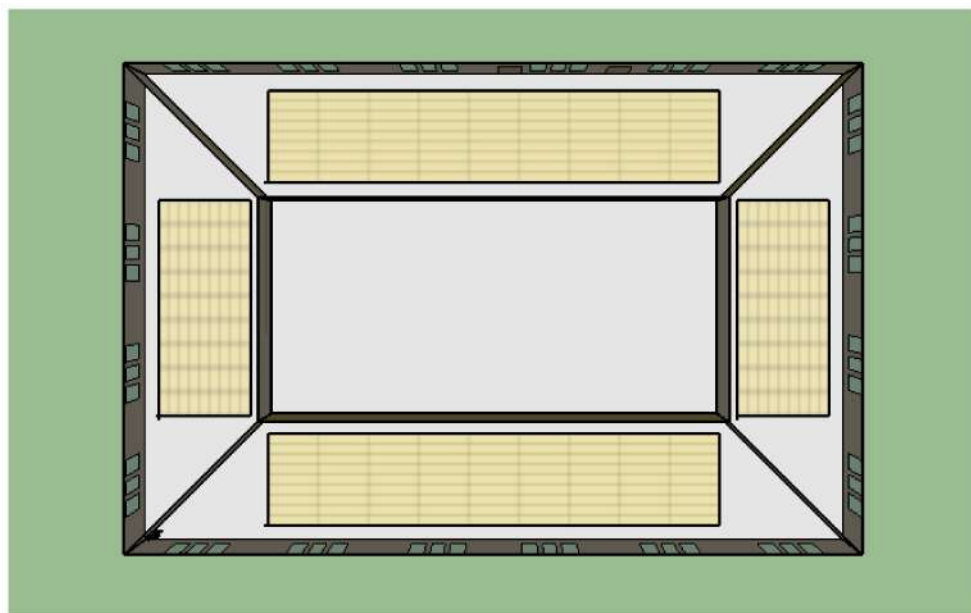


Figure 22. Illuminance maps for the whole building.

Within the illuminance map, three useful and strategic points were chosen for each room, where the limit values in which to analyse the DA were set. These points were: left point (LP), central point (CP) and right point (RP). The results of analysis are shown in the following Table 7:

The results show that the traditional window generally allowed higher DA values in both cases (300 lux and 500 lux). Considering the single zones, the traditional window made it possible to reach the desired value of DA300 (50%) in all points; LP of east zone, all points of north zone and RP of west zone showed a threshold percentage of less than 50% for DA500. Considering the entire building, the threshold of 50% was reached for both DA300 and DA500.

**Table 7.** Daylight autonomy (DA) for the reference points.

	SW-LSC_South Zone			Traditional_South Zone		
	LP	CP	RP	LP	CP	RP
DA <sub>300</sub>	56%	58%	56%	65.8%	68.5%	65.9%
DA <sub>500</sub>	43.2%	46.1%	43.6%	57.1%	61.2%	57.0%
	SW-LSC_East Zone			Traditional_East Zone		
	LP	CP	RP	LP	CP	RP
DA <sub>300</sub>	40.3%	55.0%	63.1%	57.7%	67.4%	71.5%
DA <sub>500</sub>	22.7%	37.1%	51.5%	41.5%	55.8%	63.2%
	SW-LSC_North Zone			Traditional_North Zone		
	LP	CP	RP	LP	CP	RP
DA <sub>300</sub>	42.9%	43.6%	38.9%	63.0%	62.8%	62.8%
DA <sub>500</sub>	16.3%	16.9%	11.2%	44.0%	44.4%	44.1%
	SW-LSC_West Zone			Traditional_West Zone		
	LP	CP	RP	LP	CP	RP
DA <sub>300</sub>	63.1%	59.5%	42.2%	71.6%	66.0%	58.9%
DA <sub>500</sub>	51.9%	44.3%	23.6%	63.4%	54.1%	43.3%
	SW-LSC_TOT			Traditional_TOT		
	LP	CP	RP	LP	CP	RP
DA <sub>300</sub>	50.9%	54.2%	50.1%	64.0%	65.8%	64.3%
DA <sub>500</sub>	33.2%	35.5%	31.8%	51.4%	53.7%	51.9%

Regarding the SW-LSC, considering the single one, the DA300 (50%) was reached in all points except the LP of the east zone, all points of north zone, and the RP of west zone. It was not possible to reach the 50% threshold in the case of DA500 in most points, except for the RP points of the east zone (51.5%) and the LP of the west zone (51.9%). Considering the whole building, the 50% threshold was reached in the case of DA300 but not in the case of the DA500. This was due both to the characteristic of the SW-LSC and to the presence of the light shelf, which in any case had the beneficial effect of reducing glare phenomena near the window and guaranteeing greater uniformity of the radiation inside the rooms thanks to the reflection of the same towards the ceiling. This can be observed by analysing and comparing all points (10 × 10) of the illuminance maps created. For this purpose, five categories were defined:

- low daylight (<300 lux);
- acceptable daylight (between 300 and 500 lux);
- medium daylight (between 500 and 1000 lux);
- high daylight (between 1000 and 2000 lux);
- very high daylight (>2000 lux).

The categories and ranges were chosen considering the final destination of the analysed building, which is that of an office. The results of the analysis were expressed as a percentage of points for which the illuminance value was that established in the range considered (Table 8).

Table 8 shows that in the case of the SW-LSC, there were more points whose illuminance value fell in the area between 300 and 500 lux (acceptable daylight). For the traditional window, the percentage of points which fell in the area of “high daylight” and “very high daylight” was average more than 6% and 8% when compared to the case of the SW-LSC in the same range.



**Table 8.** Percentage of points in the illuminance map with an illuminance value that falls within the defined range.

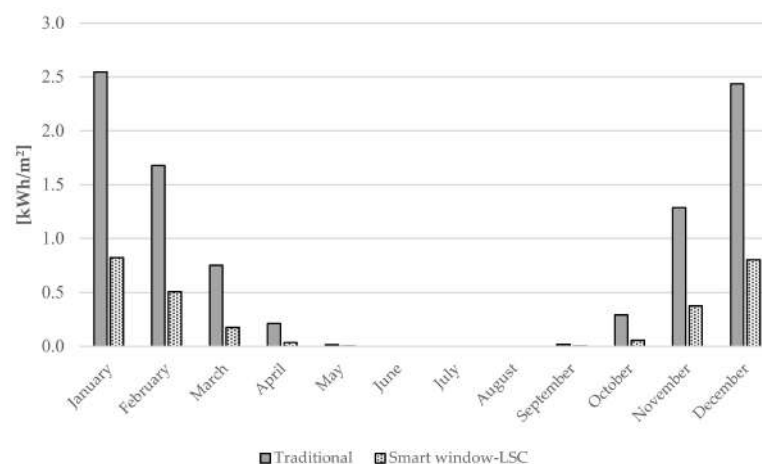
Illuminance Range	SW-LSC				Traditional Window			
	North	South	West	East	North	South	West	East
>300	48.8%	34.9%	38.6%	39.5%	29.7%	25.2%	26.7%	27.1%
300 < x < 500	28.8%	12.6%	17.5%	17.7%	18.8%	8.5%	12.3%	13%
500 < x < 1000	17.8%	24.8%	21.6%	20.8%	38.2%	17.3%	24%	24.1%
1000 < x < 2000	3.9%	18.3%	14.7%	14.3%	10.9%	26.2%	20.3%	19.1%
<2000	0.7%	9.4%	7.6%	7.7%	2.4%	22.8%	16.7%	16.7%

#### 4.4.2. Thermo-Physical Analysis

The results related to the thermo-physical analysis are shown in the following figure (Figures 23–26). First, the monthly heat balance in the small office was calculated for traditional window and SW-LSC model (Figures 23 and 24); then the daily heat balance (heating and cooling) (Figures 25 and 26) and the heat gain/loss from windows (Table 9) for the selected four days, and for the day before and after the reference day, were calculated. Results refer to the total heat balance relating to the four peripheral areas and the central area; the attic was always excluded.

**Table 9.** Heat gain and loss for traditional window and the SW-LSC scenarios.

	Cold Sunny Day (01/15)	
	Traditional Window	SW-LSC
Max heat gain	0.0055 kWh/m <sup>2</sup>	0.007 kWh/m <sup>2</sup>
Max heat loss	0.013 kWh/m <sup>2</sup>	0.0045 kWh/m <sup>2</sup>
	Cold cloudy day (12/24)	
	Traditional window	SW-LSC
Max heat gain	0.011 kWh/m <sup>2</sup>	0.003 kWh/m <sup>2</sup>
Max heat loss	0.012 kWh/m <sup>2</sup>	0.003 kWh/m <sup>2</sup>
	Warm sunny (7/22)	
	Traditional window	SW-LSC
Max heat gain	0.024 kWh/m <sup>2</sup>	0.016 kWh/m <sup>2</sup>
	Warm cloudy (8/28)	
	Traditional window	SW-LSC
Max heat gain	0.021 kWh/m <sup>2</sup>	0.011 kWh/m <sup>2</sup>

**Figure 23.** Monthly heating requirements for the two alternatives.

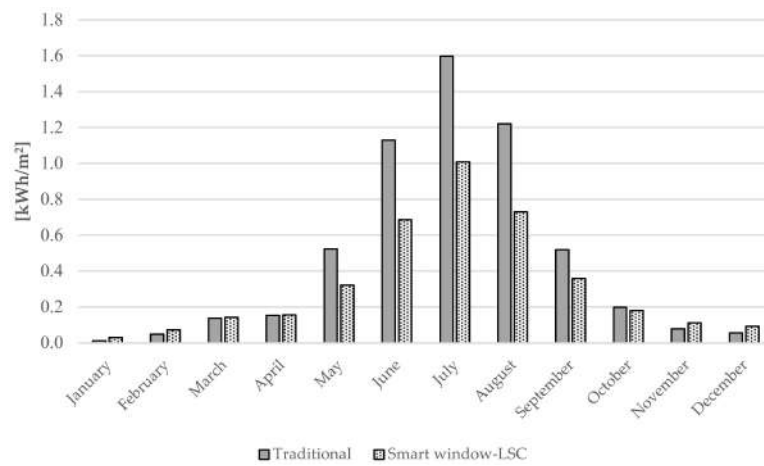
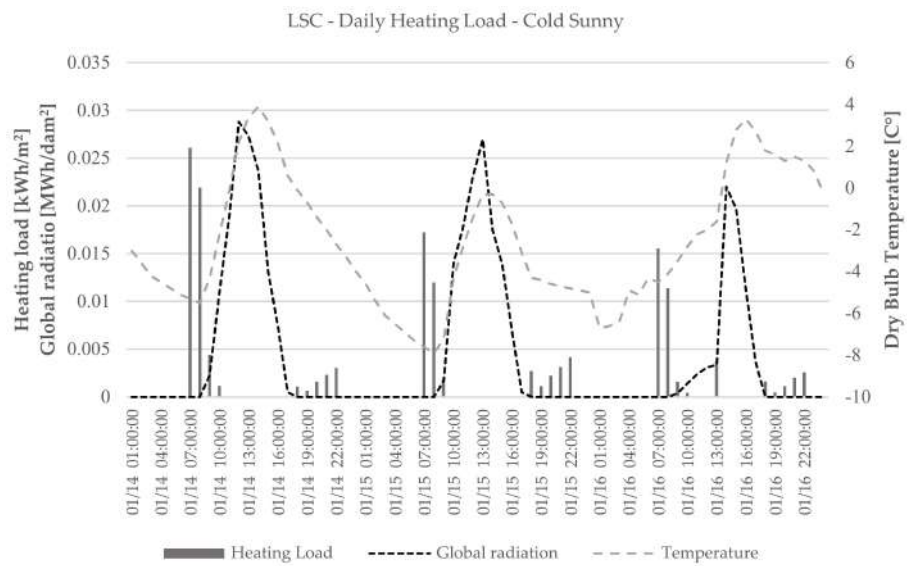
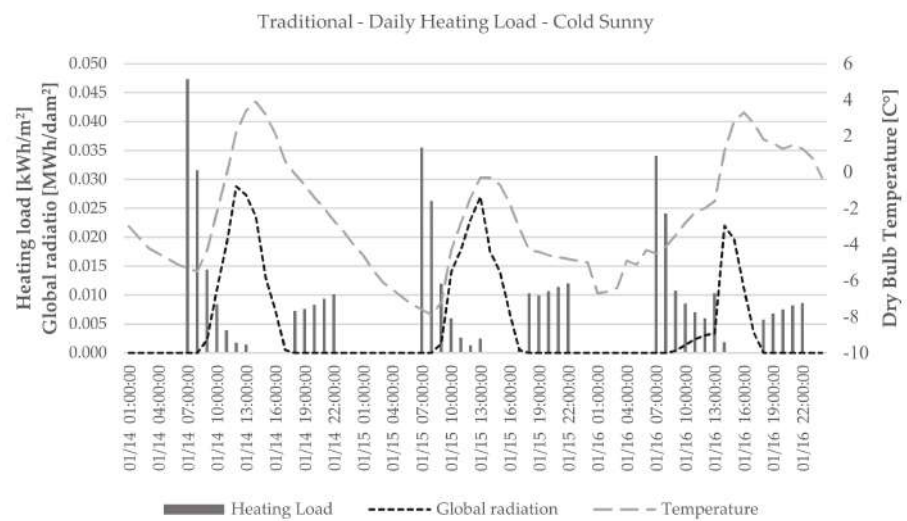


Figure 24. Monthly cooling energy uses for traditional window and SW-LSC office models.



(a)



(b)

Figure 25. Daily Heat balance for SW-LSC (a) and traditional window (b)(cold sunny period).

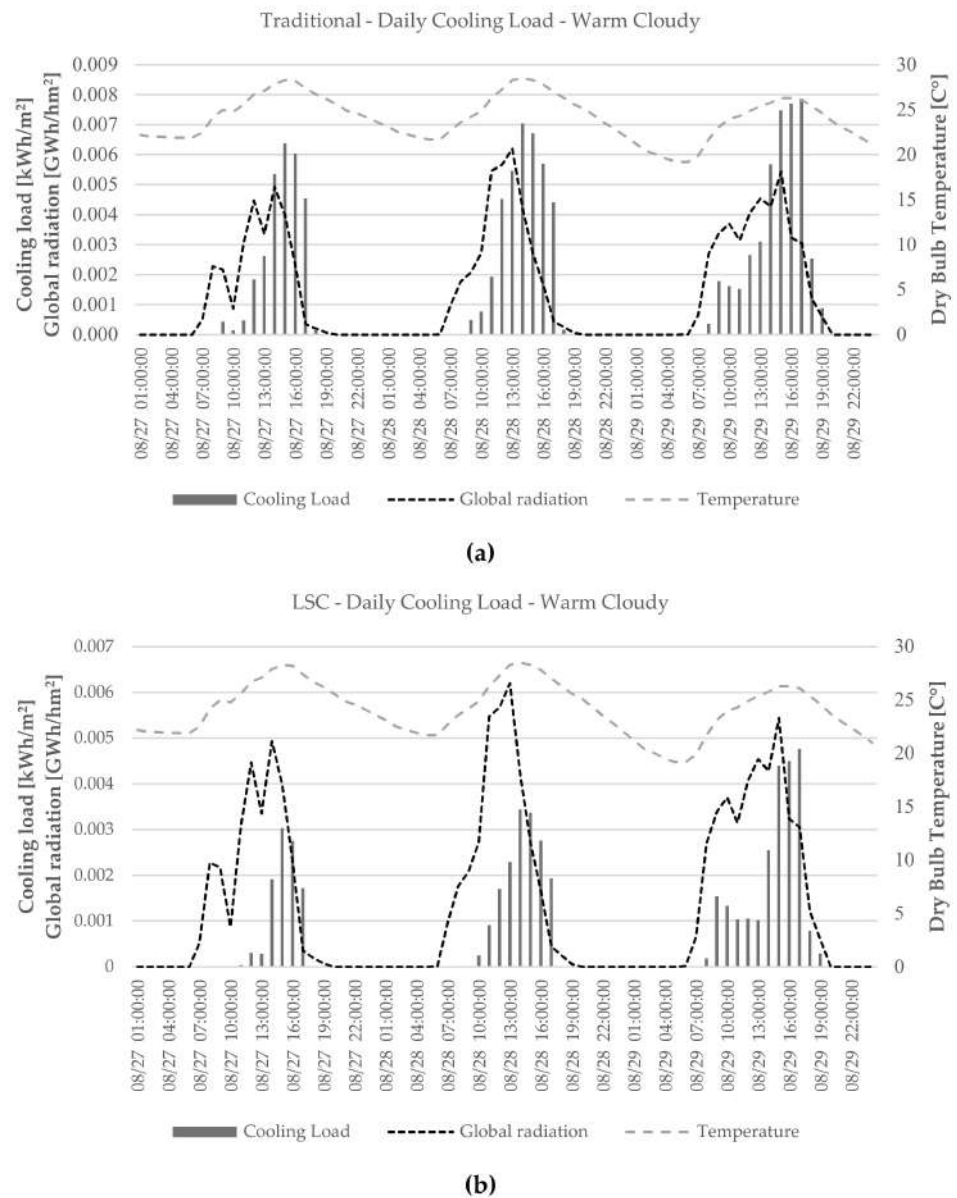


**Figure 26.** Daily heat balance for the traditional window (a) and the SW-LSC (b) (warm cloudy period).

Figure 23 shows that for the traditional window scenario, the monthly heating load was always higher than in the SW-LSC scenario (from 200 to 300%); the highest difference was recorded in January and it was equal to 1723 kWh/m<sup>2</sup>.

In the case of the cooling load, the scenario of the traditional window shows higher values (from 10 to 67%) from May to October; the highest difference was recorded in July and was equal to 0.589 kWh/m<sup>2</sup>.

The results showed that:

- During the cold sunny period (14–16 January), the maximum heating energy demand for the traditional window scenario was 0.048 kWh/m<sup>2</sup>. For the reference day (1/15) this value was 0.035 kWh/m<sup>2</sup>. The maximum heating energy demand for the SW-LSC scenario was 0.026 kWh/m<sup>2</sup> (1/14), while for the reference day it was 0.017 kWh/m<sup>2</sup>.
- During the cold cloudy period (23–25 December), the maximum heating energy demand for the traditional window scenario was 0.033 kWh/m<sup>2</sup>. For the reference day of this period (12/24), this value was 0.031 kWh/m<sup>2</sup> at 07.00. The maximum heating energy demand for the SW-LSC scenario was 0.015 kWh/m<sup>2</sup> (12/25), while for the reference day it was 0.014 kWh/m<sup>2</sup>. Thanks to a higher mean temperature (−1.6 °C), the heating energy demand was lower when compared to those of the cold

- sunny period ( $T_m = -2.6\text{ }^\circ\text{C}$ ;  $\text{MeanGlobHorRad} = 119.5\text{ W/m}^2\text{K}$ ) for both scenarios, despite the lower solar input caused by the presence of clouds ( $83.1\text{ W/m}^2\text{K}$ ).
- During the warm sunny period (21–23 July), the maximum cooling energy demand for the traditional window scenario was  $0.015\text{ kWh/m}^2$  (7/22). The maximum cooling energy demand for the SW-LSC scenario was  $0.0095\text{ kWh/m}^2$  (7/22).
  - During the warm cloudy period (27–29 August), the maximum cooling energy demand for the traditional window scenario was  $0.008\text{ kWh/m}^2$  (8/29); for the reference day (08/28) this value was  $0.007\text{ kWh/m}^2$ . The maximum cooling energy demand for the SW-LSC scenario was  $0.0048\text{ kWh/m}^2$  (8/29). For the reference day (08/28) this value was  $0.0035\text{ kWh/m}^2$ . Due to the lower solar radiation and mean temperature ( $T_m = 24.3\text{ }^\circ\text{C}$ ;  $\text{MeanGlobHorRad} = 255.7\text{ W/m}^2\text{K}$ ), the cooling energy demand was lower when compared to those of the warm sunny period ( $T_m = 27.1\text{ }^\circ\text{C}$ ;  $\text{MeanGlobHorRad} = 533.9\text{ W/m}^2\text{K}$ ) for both scenarios.

Table 9 summarizes the results for heat gains and loss in both scenarios.

#### 4.4.3. Electricity Balance

The whole building was analysed from the perspective of electricity consumption, both in the cases of the SW-LSC and of the traditional window. Furthermore, the electricity generation of the SWs-LSC installed in the south perimeter of the office building was quantified.

The electricity consumption in the office building was divided in interior lighting, external lighting, and internal equipment. As the difference of the two models (SW-LSC and Traditional) refer only on the characteristics of the windows, the electricity consumption gap between the two cases regarded only internal lighting, how can be seen in Table 10.

**Table 10.** Electrical consumption for whole building case.

	Traditional	SW-LSC
Interior Lighting	11,619.44 [kWh]	11,702.78 [kWh]
Exterior Lighting	1597.22 [kWh]	
Interior Equipment	13,716.67 [kWh]	

The use of the traditional window involved an electrical energy saving of about 83 kWh per year for internal lighting. As confirmed by daylighting tests, the perimeter areas of the building had a higher DA and this also affected electricity consumption.

For the generation of electricity by the SW-LSCs, the mathematical formulation obtained statistically in the paragraph above was exploited.

As the LSC modules also generated energy with diffuse radiation, the calculation of the generated energy referred to all the radiation that hit the upper part of the SW-LSC, also considering the diffuse component from the sky and the ground.

The analysis showed that, for the office building, the SW-LSC ( $6\text{ m}^2$  modules) facing south allowed to produce 22 kWh of electric energy. In the case of the building analysed, the shape of the roof penalized the possibility of generating energy in the months with high global radiation as shown in Figure 27.

Due to the solar position during the period from April to October, the modules were often shaded and therefore the generation of energy was reduced compared to other months (from October to March).

A further simulation was carried out to exclude the shading caused by the roof and to evaluate the full production potential for the SWs-LSC facing south. The results showed that, in this case, the electric generation was 59 kWh/year, with an increase of 62% compared to the previous case.

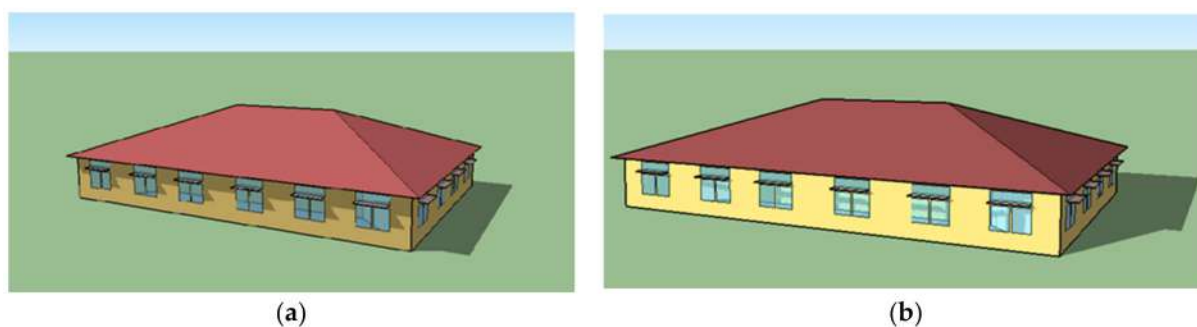


**Figure 27.** Smart windows exposed to south in the whole building model from two (a) and (b) views.

Further studies and investigations will be necessary to determine the potential for generating electricity for exposures other than the south, finding a relationship between irradiation and generation and evaluating the production for the other SWs-LSC installed in the building.

## 5. Discussion

In this section, the main results of the analyses are summarized and explained.

The LCA results showed that the most impactful components of the SW-LSC system were the window frame (above 60% contribution in most categories), the light shelf (above 20%) and the DC motors and batteries (30.74% and 36.26%, respectively in abiotic depletion but a less than 4% in all categories). The LSC modules contributed less than 5% in all impact categories.

In a life cycle perspective, it is important to stress that the aluminium frame of the SW-LSC was made up of 75% recycled material; moreover, as it was a prototype, the element can be further improved, and the design could allow the use of other less energy-intensive materials. For the same reason, the substitution, or the remotion of potentially “onerous” elements from an environmental point of view, such as the light-shelf, could be evaluated.

Regarding the daylighting performances, the validated models were used to conduct simulations for a large-building and to obtain the value of daylight autonomy in the case of a threshold of 300 lux and 500 lux. Furthermore, the study made it possible to analyse the illuminance map and to compare the distribution of light in the large-building model, both for the SW-LSC and for traditional window case. The results showed that the traditional window generally obtained higher DA values in both cases (300 lux and 500 lux) when compared to the smart window. For the traditional window, the mean DA300 for all points was 65% and DA500 was 52% while for smart window DA300 was 51.5% and DA500 was 34%. Anyway, a deeper analysis showed that illuminance values for the smart window LSC, in the area between 300 and 500 lux (acceptable daylight), were higher than of the traditional window. Consequently, the percentage of points which falls in the area of “high daylight” and “very high daylight” is on average more than 6% and 8% for the traditional window, if compared to the case of SW-LSC in the same range. These results showed that, overall, the quality and intensity of the light that filters through the LSC smart window was more suitable for the considered environment (the office) than the traditional window.

The thermo-physical analysis was based on the standard ASHRAE 90.1. The building model used refers to the small office proposed by the ASHRAE Standard 2019. The analysis made it possible to obtain the daily and monthly heat balance and the heat gains and losses in two different scenarios that involved the use of traditional windows and the SW-LSC, as the only change to the basic ASHRAE model of the small office. The results showed that, for the traditional window scenario, the monthly heating energy use was always higher than in the SW-LSC scenario (from 200 to 300%); the highest difference was recorded in January and it was equal to 1723 kWh/m<sup>2</sup>.



In the case of the cooling energy use, the scenario of the traditional window showed higher values (from 10 to 67%) and the highest difference was recorded in July and was equal to 0.589 kWh/m<sup>2</sup>.

Electrical analysis results showed that the use of the traditional window involved an electrical energy saving of about 83 kWh per year for internal lighting as the perimeter areas of the building had a higher DA and this also affected electricity consumption. Anyway, the electric generation for the smart window LSC was 59 kWh/year for the site of Novara and it can be expected that this result can be further increased in locations with an average radiation higher than that of this study. As a result, the higher electricity consumption can certainly be counterbalanced by increased production thanks to the LSC modules. To this end, further studies are needed to quantify the impact of the reference geographical location.

## 6. Conclusions

In this study, a smart window prototype with integrated LSC modules was examined, focusing on environmental, lighting, thermal and electrical performance.

The environmental analysis identified hot-spots, characterized by the higher impacts, that could be taken into account for future design strategies of the system.

The experiment setup obtained the illuminance level inside the rooms, where the two windows were installed, through a monitoring study. The simulation of the lighting performance started after the creation of the two rooms model and the two windows models through an illuminance map that contained the points where the real measurements were taken. After the calibration process, based on the uncertainties of some model parameters, the results of the simulations were compared with those of the measurements and the percentage error between the two values (simulated and measured) was calculated. The results showed that the models created approximate with good accuracy (generally with an error of less than 10%) the characteristics of the two windows and allowed to validate the experimental procedure for obtaining and developing the data obtained.

After validation of the models in a test building, a series of analyses were conducted to evaluate the thermal, electrical and optical performance of the SW-LSC in a larger building (office). Although the results, especially those of thermos-physical analysis, can be predictable, considering the better characteristics of the glass and the frame of the smart window compared to the traditional window, the study quantified the advantages of using the SW-LSC instead of a traditional window. The importance of these results lies in the innovation of the device and in the lack of references in the literature for this new technology; these results can be used for further investigations and for comparisons with other similar technologies suitable for the same type of application.

The analysis of electrical performance was performed starting with the collection of generation and consumption data monitored during the experimental study. Through a statistical approach conducted on these data, the relationship between irradiation and energy generation was obtained for the SW-LSC prototype installed in the test building. Subsequently, this relationship was used on the large-building to determine the generation of the SW-LSCs installed in the building and exposed along the same direction as the experimental tests. Finally, a comparison was made between the consumption of internal lighting in the case of the SW-LSC and the traditional window. The electrical performances evaluation showed that further improvements are necessary for LSC technology, in particular in their efficiency, as for certain locations (such as the reference one in the study) in which solar radiation does not reach high average values during the year, the production of energy only allows to balance the higher consumption due to a lower illumination of indoor environments.

In conclusion, considering the mixed nature of the SW-LSC prototype, we believe that the procedure presented in this study is an effective path to evaluate the performance of this new technology, also allowing a comparison with other semi-transparent PV technologies and smart glasses/smart windows, in the perspective of a real staircase of the building.

Furthermore, this study provides useful information to plan energy renovation strategies for existing buildings to save on energy costs and to reduce the environmental effects of the building, involving a critical element such as windows.

**Author Contributions:** Conceptualization, all authors; methodology, all authors; software, F.G., V.M.; validation, L.B., D.T., M.B. and F.G.; formal analysis, V.M., S.L. investigation, all authors; resources, L.B., M.C.; data curation, L.B., D.T., M.B., V.M.; writing—original draft preparation, V.M.; writing—review and editing, all authors; visualization, F.G., S.L.; supervision, L.B., M.C.; project administration, L.B., M.C., S.L. All authors have read and agreed to the published version of the manuscript.

**Funding:** This research was co-funded with the resources of the Italian Operative Programme for Research and Innovation 2014–2020 (CCI 2014IT16M2OP005), European Social Fund, Action I.1 “Innovative PhD with industrial characterization”.

**Institutional Review Board Statement:** Not applicable.

**Informed Consent Statement:** Not applicable.

**Data Availability Statement:** Not applicable.

**Conflicts of Interest:** The authors declare no conflict of interest.

## References

1. Ibn-mohammed, T. Application of Mixed-Mode Research Paradigms to the Building Sector: A Review and Case Study Towards Decarbonising the Built and Natural Environment. *Sustain. Cities Soc.* **2017**, *35*, 692–714. [\[CrossRef\]](#)
2. Cellura, M.; Guarino, F.; Longo, S.; Tumminia, G. Climate Change and the Building Sector: Modelling and Energy Implications to an Office Building in Southern Europe. *Energy Sustain. Dev.* **2018**, *45*, 46–65. [\[CrossRef\]](#)
3. Guarino, F.; Croce, D.; Tinnirello, I.; Cellura, M. Data Fusion Analysis Applied to Different Climate Change Models: An Application to the Energy Consumptions of a Building Office. *Energy Build.* **2019**, *196*, 240–254. [\[CrossRef\]](#)
4. Bilgen, S. Structure and Environmental Impact of Global Energy Consumption. *Renew. Sustain. Energy Rev.* **2014**, *38*, 890–902. [\[CrossRef\]](#)
5. Tumminia, G.; Guarino, F.; Longo, S.; Ferraro, M.; Cellura, M.; Antonucci, V. Life Cycle Energy Performances and Environmental Impacts of a Prefabricated Building Module. *Renew. Sustain. Energy Rev.* **2018**, *92*, 272–283. [\[CrossRef\]](#)
6. Guarino, F.; Cassarà, P.; Longo, S.; Cellura, M.; Ferro, E. Load Match Optimisation of a Residential Building Case Study: A Cross-Entropy Based Electricity Storage Sizing Algorithm. *Appl. Energy* **2015**, *154*. [\[CrossRef\]](#)
7. Hachem-Vermette, C.; Guarino, F.; La Rocca, V.; Cellura, M. Towards Achieving Net-Zero Energy Communities: Investigation of Design Strategies and Seasonal Solar Collection and Storage Net-Zero. *Sol. Energy* **2018**, *192*, 169–185. [\[CrossRef\]](#)
8. Fichera, A.; Marrasso, E.; Sasso, M.; Volpe, R. Energy, Environmental and Economic Performance of an Urban Community Hybrid Distributed Energy System. *Energies* **2020**, *13*, 2545. [\[CrossRef\]](#)
9. Longo, S.; Guarino, F.; Ferraro, M.; Brunaccini, G.; Aloisio, D.; Sergi, F.; Tumminia, G.; Cellura, S.; Antonucci, V. Grid Interaction and Environmental Impact of a Net Zero Energy Building. *Energy Convers. Manag.* **2020**, *203*, 112228. [\[CrossRef\]](#)
10. Tällberg, R.; Petter, B.; Loonen, R.; Gao, T.; Hamdy, M. Comparison of the Energy Saving Potential of Adaptive and Controllable Smart Windows: A State-Of-The-Art Review and Simulation Studies of Thermochromic, Photochromic and Electrochromic Technologies. *Sol. Energy Mater. Sol. Cells* **2019**, *200*, 109828. [\[CrossRef\]](#)
11. Li, D.H.W. A Review of Daylight Illuminance Determinations and Energy Implications. *Appl. Energy* **2010**, *87*, 2109–2118. [\[CrossRef\]](#)
12. Das, A.; Paul, S.K. Artificial Illumination during Daytime in Residential Buildings: Factors, Energy Implications and Future Predictions. *Appl. Energy* **2015**, *158*, 65–85. [\[CrossRef\]](#)
13. Anaya, M.; Lozano, G.; Calvo, E.A.; Miguez, H. ABX3 Perovskites for Tandem Solar Cells. *Joule* **2017**, *1*, 769–793. [\[CrossRef\]](#)
14. Zhang, T.; Wang, M.; Yang, H. A Review of the Energy Performance and Life-Cycle Assessment of Building-Integrated Photovoltaic (BIPV) Systems. *Energies* **2018**, *11*, 3157. [\[CrossRef\]](#)
15. Sun, Y.; Shanks, K.; Baig, H.; Zhang, W.; Hao, X.; Li, Y.; He, B.; Wilson, R.; Liu, H.; Sundaram, S.; et al. Integrated CdTe PV Glazing into Windows: Energy and Daylight Performance for Different Window-To-Wall Ratio. *Energy Procedia* **2019**, *158*, 3014–3019. [\[CrossRef\]](#)
16. Kapsis, K.; Athienitis, A.K. A Study of the Potential Benefits of Semi-transparent Photovoltaics in Commercial Buildings. *Sol. Energy* **2015**, *115*, 120–132. [\[CrossRef\]](#)
17. Frattolillo, A.; Loddo, G.; Mastino, C.C.; Baccoli, R. Heating and Cooling Loads with Electrochromic Glazing in Mediterranean Climate. *Energy Build.* **2019**, *201*, 174–182. [\[CrossRef\]](#)
18. Wu, L.Y.L.; Zhao, Q.; Huang, H.; Lim, R.J. Sol-Gel Based Photochromic Coating for Solar Responsive Smart Window. *Surf. Coatings Technol.* **2017**, *320*, 601–607. [\[CrossRef\]](#)

19. Aste, N.; Leonforte, F.; Piccolo, A. Color Rendering Performance of Smart Glazings for Building Applications. *Sol. Energy* **2018**, *176*, 51–61. [[CrossRef](#)]
20. Warwick, M.E.A.; Ridley, I.; Binions, R. The Effect of Variation in the Transition Hysteresis Width and Gradient in Thermochromic Glazing Systems. *Sol. Energy Mater. Sol. Cells* **2015**, *140*, 253–265. [[CrossRef](#)]
21. Ye, H.; Long, L.; Zhang, H.; Gao, Y.; Kang, L.; Chen, Z. The Demonstration and Simulation of the Application Performance of the Vanadium Dioxide Single Glazing. *Sol. Energy Mater. Sol. Cells* **2013**, *117*, 168–173. [[CrossRef](#)]
22. Yang, J.; Xu, Z.; Ye, H.; Xu, X.; Wu, X.; Wang, J. Performance Analyses of Building Energy on Phase Transition Processes of VO<sub>2</sub> Windows with an Improved Model. *Appl. Energy* **2015**, *159*, 502–508. [[CrossRef](#)]
23. Costanzo, V.; Evola, G.; Marletta, L. Thermal and Visual Performance of Real and Theoretical Thermochromic Glazing Solutions for Office Buildings. *Sol. Energy Mater. Sol. Cells* **2016**, *149*, 110–120. [[CrossRef](#)]
24. Rezaei, S.D.; Shannigrahi, S.; Ramakrishna, S. A Review of Conventional, Advanced, and Smart Glazing Technologies and Materials for Improving Indoor Environment. *Sol. Energy Mater. Sol. Cells* **2017**, *159*, 26–51. [[CrossRef](#)]
25. Reynisson, H.E. Energy Performance of Dynamic Windows in Different Climates. Master's Thesis, KTH, School of Architecture and the Built Environment (ABE), Civil and Architectural Engineering, Building Technology, Stockholm, Sweden, 2015.
26. Ajaji, Y.; André, P. Thermal Comfort and Visual Comfort in an Office Building Equipped with Smart Electrochromic Glazing: An Experimental Study. *Energy Procedia* **2015**, *78*, 2464–2469. [[CrossRef](#)]
27. Aste, N.; Buzzetti, M.; Del Pero, C.; Leonforte, F.; Eni S.p.A./Polytechnic University of Milan, Milan, Italy. "Progettazione Definitiva e Redazione del Piano di Industrializzazione di una Smart Window Integrata con Componenti LSC (Concentratori Solari Luminescenti) Secondo Rapporto Intermedio". 2017; 5, 1–47, Unpublished internal company document.
28. Aste, N.; Buzzetti, M.; Del Pero, C.; Fusco, R.; Testa, D.; Leonforte, F. Visual Performance of Yellow, Orange and Red LSCs Integrated in a Smart Window. *Energy Procedia* **2017**, *105*, 967–972. [[CrossRef](#)]
29. Aste, N.; Buzzetti, M.; Del Pero, C.; Fusco, R.; Leonforte, F.; Testa, D. Triggering a Large Scale Luminescent Solar Concentrators Market: The Smart Window Project. *J. Clean. Prod.* **2019**, *219*, 35–45. [[CrossRef](#)]
30. Aste, N.; Buzzetti, M.; Del Pero, C.; Leonforte, F.; Eni S.p.A./Polytechnic University of Milan, Milan, Italy. "Progettazione definitiva e redazione del piano di industrializzazione di una Smart Window integrata con componenti LSC (Concentratori Solari Luminescenti) Primo Rapporto Intermedio". 2017; 4, 1–33, Unpublished internal company document.
31. Aste, N.; Buzzetti, M.; Del Pero, C.; Leonforte, F.; Eni S.p.A./Polytechnic University of Milan, Milan, Italy. "Sviluppo Tecnologico di Componenti LSC Destinati all'Integrazione Edilizia e Attività di Supporto allo Sviluppo Industriale". 2015; 1, 1–18, Unpublished internal company document.
32. Aste, N.; Buzzetti, M.; Del Pero, C.; Leonforte, F.; Eni S.p.A./Polytechnic University of Milan, Milan, Italy. "Sviluppo Tecnologico di Componenti LSC Destinati all'Integrazione Edilizia e Attività di Supporto allo Sviluppo Industriale Secondo Rapporto Intermedio". 2016; 2, 1–105, Unpublished internal company document.
33. Aste, N.; Del Pero, C.; Tagliabue, L.C.; Leonforte, F.; Testa, D.; Fusco, R. Performance Monitoring and Building Integration Assessment of Innovative LSC Components. In Proceedings of the 5th International Conference on Clean Electrical Power: Renewable Energy Resources Impact ICCEP, Taormina, Italy, 16–18 June 2015; pp. 129–133. [[CrossRef](#)]
34. Aste, N.; Buzzetti, M.; Del Pero, C.; Leonforte, F.; Eni S.p.A./Polytechnic University of Milan, Milan, Italy. "Progettazione Definitiva e Redazione del Piano di Industrializzazione di Una Smart Window Integrata con Componenti LSC (Concentratori Solari Luminescenti) Rapporto Finale". 2017; 6, 1–99, Unpublished internal company document.
35. Aste, N.; Buzzetti, M.; Del Pero, C.; Leonforte, F.; Eni S.p.A./Polytechnic University of Milan, Milan, Italy. "Progettazione Definitiva e Redazione del Piano di Industrializzazione di Una Smart Window Integrata con Componenti LSC (Concentratori Solari Luminescenti) Rapporto Finale". 2018; 7, 1–33, Unpublished internal company document.
36. Aste, N.; Buzzetti, M.; Del Pero, C.; Leonforte, F.; Eni S.p.A./Polytechnic University of Milan, Milan, Italy. "Supporto alla Pre-Commercializzazione di Componenti LSC (Concentratori Solari Luminescenti) Destinati all'Integrazione Edilizia Rapporto Definitivo". 2019; 8, 1–68, Unpublished internal company document.
37. Aste, N.; Buzzetti, M.; Del Pero, C.; Leonforte, F.; Eni S.p.A./Polytechnic University of Milan, Milan, Italy. "Sviluppo Tecnologico di Componenti LSC Destinati all'Integrazione Edilizia e Attività di Supporto allo Sviluppo Industriale Rapporto Finale". 2016; 3, 1–188, Unpublished internal company document.
38. Muteri, V. Energy Evaluation and Life Cycle Assessment of an Innovative Building Integrated Technology: The Smart Window—Luminescent Solar Concentrator. Ph.D. Thesis, University of Palermo, Palermo, Italy, 2001.
39. Attia, S.; Hamdy, M.; Carlucci, S.; Pagliano, L.; Bucking, S.; Hasan, A. Building Performance Optimization of Net Zero-Energy Buildings. In *Modeling, Design, and Optimization of Net-Zero Energy Buildings*; Wilhelm Ernst & Sohn: Berlin, Germany, 2015; pp. 175–206. [[CrossRef](#)]
40. Kesik, T. Solar Design Days: A Tool for Passive Solar House Design. *ASHRAE Trans.* **2014**, *120*, 101.